Agricultural and Forest Meteorology 323 (2022) 109059

Contents lists available at ScienceDirect

Agricultural and Forest Meteorology

journal homepage: www.elsevier.com/locate/agrformet

Calibration and characterisation of four chlorophyll meters and transmittance spectroscopy for non-destructive estimation of forest leaf chlorophyll concentration

Luke A. Brown *, Owen Williams, Jadunandan Dash

School of Geography and Environmental Science, University of Southampton, Highfield, Southampton, SO17 1BJ, UK

ARTICLE INFO

Editor: Timo Vesala

Keywords:
atLEAF
CCI
CCM-200
Chlorophyll
MultispeQ
SPAD

ABSTRACT

Chlorophyll meters enable efficient and non-destructive estimation of leaf chlorophyll concentration (LCC), but require calibration against destructively-determined values to provide an absolute quantity that is comparable between different studies and species. Well-established instruments can provide accurate LCC estimates, but the performance of recent low-cost devices is less clear. Questions also remain over the choice of generic or species-specific calibration functions. Additionally, little attention has been paid to transmittance spectroscopy, which offers substantially increased spectral sampling, as a potential alternative. We investigated the well-established Konica Minolta SPAD-502+ and Opti-Sciences CCM-200 instruments and the low-cost atLEAF CHL PLUS and PhotosynQ MultispeQ V1.0 devices for non-destructive estimation of forest LCC. We calibrated each chlorophyll meter against destructively-determined LCC values for eight temperate deciduous broadleaf forest species, and characterised relationships between the different instruments. We also assessed whether transmittance spectroscopy could provide improved accuracy. All investigated chlorophyll meters demonstrated similarly strong relationships with destructively-determined LCC, indicating that once calibrated, even the low-cost devices represent a suitable choice for non-destructive forest LCC estimation. With the exception of oak, chlorophyll meter – LCC relationships were consistent between species, indicating that for these species, a generic calibration function may be suitable depending on required accuracy. Specifically, LCC values provided by the generic calibration functions fell within the prediction uncertainties of species-specific calibration functions for most considered species. The generic calibration functions explained between 2% and 16% less variation in LCC than the species-specific calibration functions, resulting in a mean increase in RMSE (NRMSE) of just 0.01 g m^{-2} to 0.02 g m^{-2} (2% to 5%). Transmittance spectroscopy was able to provide improved performance over the chlorophyll meters, indicating that they may miss some relevant spectral information at blue and green wavelengths. However, this improved performance comes at the expense of reduced practicality in the field.

1. Introduction

Chlorophyll is the key photosynthetic pigment in plants, and plays a crucial role in determining the physiological status of vegetation. Leaf chlorophyll concentration (LCC), which describes the quantity of chlorophyll per unit leaf area or unit leaf mass, is a sensitive indicator of plant health, responding to the availability of water, nutrients such as nitrogen, and other physical and environmental factors (Clevers and Gitelson, 2013; Lichtenthaler et al., 1998). As such, information on the spatiotemporal variability of LCC is valuable in the management of vegetated landscapes, providing a useful measure of vegetation vigour that can inform necessary interventions. In the context of agriculture and forestry, LCC measurements can be used to infer nitrogen status and serve as an indicator of other forms of plant stress such as water deficit and the presence of pests and pathogens, whilst also providing a proxy for productivity (Bonneville and Fyles, 2006; Percival et al., 2008; van den Berg and Perkins, 2004). Information from such measurements can, therefore, enable the targeted application of fertilisers, irrigation, and pesticides (Blackmer and Schepers, 1995; Peng et al., 1996; Varvel et al., 1997), and support decisions related to harvesting and felling operations.

Traditionally, the measurement of LCC involved destructive

* Corresponding author.
E-mail address: l.a.brown@soton.ac.uk (L.A. Brown).

https://doi.org/10.1016/j.agrformet.2022.109059
Received 17 December 2021; Received in revised form 7 June 2022; Accepted 13 June 2022
Available online 24 June 2022

sampling of leaves, transportation of the samples to a laboratory, extraction of chlorophyll using a solvent, and subsequent chemical analysis (Parry et al., 2014; Richardson et al., 2002; Wellburn, 1994). To address the time-consuming and laborious nature of this process, a variety of transmittance-based chlorophyll meters have been developed over the past few decades, eliminating the need for destructive sampling and enabling rapid in situ estimation of LCC. All are based on similar measurement principles, making use of narrowband light emitting diodes (LEDs) and a photodiode to determine an index based on the transmittance of the leaf at multiple wavelengths (Dong et al., 2019; Monje and Bugbee, 1992; Parry et al., 2014; Uddling et al., 2007). A less widely used approach involves fluorescence-based chlorophyll meters, which adopt a blue LED as an excitation source, and use a pair of detectors equipped with narrowband filters to determine the ratio of chlorophyll fluorescence at two different wavelengths (Gitelson et al., 1999).

Despite the efficiency of chlorophyll meters, it is important to recognise that their outputs represent a relative quantity that is related, but not equivalent, to LCC. Previous work has demonstrated that transmittance-based chlorophyll meter outputs are influenced by the non-uniform distribution of chlorophyll within a leaf (and the resulting sieve and detour effects, whereby light may pass through a leaf without encountering any pigments, or be scattered by its internal structure) (Cerovic et al., 2012; Markwell et al., 1995; Monje and Bugbee, 1992; Nauš et al., 2010; Parry et al., 2014; Uddling et al., 2007). As a result, to derive LCC in absolute units, calibration against destructively-determined LCC values is necessary. A wide range of studies have demonstrated that, when calibrated, chlorophyll meters such as the Konica Minolta SPAD-502+, Opti-Sciences CCM-200, Apogee Instruments MC-100, and METOS DUALEX can provide accurate estimates of LCC for various plant species (Cerovic et al., 2012; Coste et al., 2010; Demarez et al., 1999; Markwell et al., 1995; Parry et al., 2014; Percival et al., 2008; Richardson et al., 2002; Steele et al., 2008; Uddling et al., 2007). Due to variations in factors such as leaf structure, surface characteristics, water content, and the presence of other pigments that could confound the optical measurement, species-specific calibration functions are often recommended (Dash et al., 2010; Demarez et al., 1999; Dong et al., 2019; Percival et al., 2008; Uddling et al., 2007). Nevertheless, some studies have proposed generic or 'consensus' calibration functions (Cerovic et al., 2012; Coste et al., 2010; Parry et al., 2014). In the case of deciduous broadleaf forest species, it remains unclear if species-specific calibration functions are a strict necessity.

In addition to well-established instruments, a number of low-cost chlorophyll meters have become available in recent years, claiming to offer similar functionality at a substantially reduced price (e.g. $350 to $625 vs. > $1,700). Examples include the atLEAF CHL PLUS and PhotosynQ MultispeQ V1.0. If these devices can offer comparable results, they could open up opportunities for more widespread use by researchers and citizen scientists (Kuhlgert et al., 2016; Newman et al., 2012), and the wealth of additional collected data could facilitate new insights in plant science. However, few comprehensive assessments of the performance of low-cost chlorophyll meters have so far been carried out, whilst published calibration functions are lacking, particularly for deciduous broadleaf forest species (Cahyo et al., 2020; Kuhlgert et al., 2016; Mendoza-Tafolla et al., 2019; Zhu et al., 2012). As such, there is a clear need for further and more thorough investigation of these devices.

Notwithstanding their utility, by virtue of their design, transmittance-based chlorophyll meters are typically restricted to just two spectral bands, meaning that relevant information contained in other parts of the spectrum is disregarded. Offering full sampling of the visible and near-infrared regions, reflectance spectroscopy has been adopted (primarily by researchers) as an alternative non-destructive means of LCC estimation. Using spectrally-resolved measurements of leaf reflectance, a number of reflectance-based indices have been related to destructively-determined LCC. At the leaf level, such indices, which are typically developed by selecting optimal bands, have in some cases demonstrated improved relationships with destructively-determined LCC than achieved using chlorophyll meters (Gitelson et al., 2003; le Maire et al., 2008; Richardson et al., 2002; Sims and Gamon, 2002; Steele et al., 2008). These reflectance-based techniques are also of particular interest at the canopy and landscape scales, since canopy reflectance can be quantified using multispectral and hyperspectral sensors on-board a range of tower-based (Gamon et al., 2006b, 2006a; Hilker et al., 2007; Leuning et al., 2006; Meroni et al., 2011; Sakowska et al., 2015; Tagesson et al., 2015; Woodgate et al., 2020), airborne (Atkins et al., 2020; Berra et al., 2017; Fawcett et al., 2020; Gao et al., 2009; Revill et al., 2019; Thompson et al., 2015; Wang et al., 2021), and satellite-based (Claverie et al., 2018; Origo et al., 2020; Vermote et al., 2016; Wolters et al., 2021) platforms.

Whilst considerable research into reflectance-based LCC estimation has been conducted, less attention has been paid to transmittance spectroscopy, despite its measurement principle being so similar to that of the chlorophyll meters (Carter and Knapp, 2001; Spafford et al., 2021; Sun et al., 2018; Wang et al., 2015; Yamada and Fujimura, 1991). By adopting transmittance as opposed to reflectance spectroscopy, the perturbing effects of specular reflectance from the surface of the leaf, which confounds LCC estimation for waxy leaves and leaves with a large number of hairs (Gitelson et al., 2003; Sims and Gamon, 2002), could largely be eliminated. Similarly, by using an active source of illumination, uncertainties related to the characterisation of irradiance at lower levels of the canopy (as opposed to the top of canopy, where irradiance is typically measured in passive reflectance spectroscopy) could be avoided (Moncholi-Estornell et al., 2021) (though such a source could also be used for active reflectance spectroscopy). When compared to two-band chlorophyll meters, the increased spectral sampling afforded by transmittance spectroscopy has the potential to provide more accurate estimates of LCC, especially when coupled with the high quality, signal-to-noise, and sensitivity characteristics of research-grade spectroradiometers. Finally, by leveraging the full-spectrum capabilities of the approach, information on which wavelengths are most informative for LCC estimation could provide insight for future development and improvement of existing chlorophyll meter designs (though it is worth recognising that any improvements might be constrained by the cost and availability of appropriate LEDs).

Using data collected for eight temperate deciduous broadleaf forest species, in this study, we calibrate and characterise four chlorophyll meters, including two well-established instruments and two low-cost devices. Using the same leaf samples to ensure a fair comparison, we provide a comprehensive assessment of chlorophyll meter performance in estimating destructively-determined LCC, and characterise the relationships between the different chlorophyll meter outputs. We also assess transmittance spectroscopy as a potential alternative for non-destructive LCC estimation. In doing so, we address the following research questions:

1 What are the relationships between chlorophyll meter outputs and destructively-determined LCC for various temperate deciduous broadleaf forest species, and are these relationships species-specific?
2 Can low-cost chlorophyll meters provide comparable performance to well-established instruments?
3 How do the outputs of the different chlorophyll meters relate to each other?
4 Can transmittance spectroscopy provide more accurate non-destructive estimates of forest LCC than can be achieved by chlorophyll meters?

2. Materials and methods

2.1. Study sites and leaf sampling

Leaf sampling was carried out on five dates throughout the spring

Table 1
Overview of leaf sampling carried out in the spring and summer of 2021.

Date	Site	Species	Samples
14/05/2021	Highfield	Beech, silver birch, hawthorn, hazel, red maple, oak, sycamore	105
20/05/2021	Wytham Woods	Ash, beech, silver birch, hawthorn, hazel, sycamore	90
03/06/2021	Highfield	Ash, beech, silver birch, hawthorn, hazel, red maple, oak, sycamore	120
25/06/2021	Highfield	Ash, beech, silver birch, hawthorn, hazel, red maple, oak, sycamore	120
11/08/2021	Highfield	Ash, red maple, oak	45

Table 2
Details of investigated chlorophyll meters.

Chlorophyll meter	Wavelengths used (nm)	Approximate cost ($)
atLEAF CHL PLUS	640, 940	350
Konica Minolta SPAD-502+	650, 940	4,150
Opti-Sciences CCM-200	653, 931	1,700
PhotosynQ MultispeQ V1.0	655, 950	625

and summer of 2021 at the University of Southampton's Highfield Campus (50.9357°N, 1.3966°W), and Wytham Woods, Oxfordshire, United Kingdom (51.7734°N, 1.3384°W) (Table 1). Across these dates, a total of 480 leaf samples were collected, covering ash (*Fraxinus excelsior*), beech (*Fagus sylvatica*), silver birch (*Betula pendula*), hawthorn (*Crataegus monogyna*), hazel (*Corylus avellana*), red maple (*Acer rubrum*), oak (*Quercus robur*), and sycamore (*Acer pseudoplatanus*). The timing of data collection was designed to capture the gradient of low LCC at the start of the growing season through to peak LCC in the summer (and associated phenological changes in leaf optical properties) (Demarez et al., 1999; Dillen et al., 2012; Koike, 1990; Noda et al., 2021). On each date and for each species sampled, 15 sunlit leaves were selected to span as wide a range of LCC as possible (assessed visually on the basis of leaf colour), yielding a total of 60 samples per species. Provided leaves are sampled from the sunlit portion of the crown, previous work has demonstrated that biochemical, structural, and spectral properties are unaffected by branch azimuthal orientation (Lhotáková et al., 2007). Leaves were placed in individual polyethylene sample bags and refrigerated until chlorophyll meter and transmittance measurements were made.

2.2. Chlorophyll meters

For the purposes of this study, four chlorophyll meters were investigated, including the well-established Konica Minolta SPAD-502+ and Opti-Sciences CCM-200 instruments, in addition to the low-cost atLEAF CHL PLUS and PhotosynQ MultispeQ V1.0 devices (Table 2). The Konica Minolta SPAD-502+ is the most widely used chlorophyll meter, having been developed in the late 1980s and adopted in a wide range of operational and scientific applications (Dong et al., 2019; Monje and Bugbee, 1992; Parry et al., 2014; Uddling et al., 2007). Using the ratio of incident and transmitted radiation at 650 nm and 940 nm, the instrument provides a relative value (M) that is proportional to LCC as

$$M = k \log \frac{I_{0_{650}}\, I_{940}}{I_{650}\, I_{0_{940}}} + C = k \log \frac{T_{940}}{T_{650}} + C \quad (1)$$

where I_{650}, I_{940}, $I_{0_{650}}$, and $I_{0_{940}}$ are the incident and transmitted radiation at 650 nm and 940 nm, respectively, whilst T_{650} and T_{940} are the transmittance at 650 nm and 940 nm, respectively (Fig. 1), and k and C represent gain and offset coefficients that are, at present, undisclosed by Konica Minolta (Cerovic et al., 2012; Dong et al., 2019; Markwell et al., 1995; Nauš et al., 2010; Parry et al., 2014; Uddling et al., 2007).

The atLEAF CHL PLUS and PhotosynQ MultispeQ V1.0 are based on the measurement principles of the Konica Minolta SPAD-502+, with some minor differences. For example, instead of LEDs centred at 650 nm and 940 nm, the atLEAF CHL PLUS uses LEDs centred at 640 nm and 940 nm (FT Green, 2018), whilst the PhotosynQ MultispeQ V1.0 uses LEDs centred at 655 nm and 950 nm (PhotosynQ, 2021a) (Fig. 1). Note that although the latter instrument has been superseded by the PhotosynQ MultispeQ V2.0, its critical optical components (i.e. the photodiode and LEDs) remain the same (PhotosynQ, 2021b). In an attempt to increase its dynamic range for thick leaves and leaves with high LCC, the latter instrument also uses a series of measurements over progressively increasing light intensities (Kuhlgert et al., 2016). Unlike the atLEAF CHL PLUS and PhotosynQ MultispeQ V1.0, the Opti-Sciences CCM-200 adopts a different measurement equation, along with LEDs centred at 653 nm and 931 nm (Fig. 1). It determines the so-called 'chlorophyll content index' (CCI) as

$$CCI = \frac{I_{0_{653}}\, I_{931}}{I_{653}\, I_{0_{931}}} = \frac{T_{931}}{T_{653}} \quad (2)$$

where I_{653}, I_{931}, $I_{0_{653}}$, and $I_{0_{931}}$ are the incident and transmitted radiation at 653 nm and 931 nm, respectively, whilst T_{653} and T_{931} represent the transmittance at 653 nm and 931 nm, respectively (Dong et al., 2019; Parry et al., 2014).

Although not explicitly investigated in this study, it is worth noting that the Apogee Instruments MC-100 is based on the same design and hardware as the Opti-Sciences CCM-200 (retailing at a similar cost), and also outputs CCI values, making our results equally applicable to this instrument. Note, however, that the Apogee Instruments MC-100 is unique in terms of its software, which currently incorporates 31 predefined calibration functions covering a range of crops and deciduous species (in addition to a generic calibration function for use when an appropriate species-specific calibration function is not available). This enables a direct read-out of LCC the device itself, removing the requirement for measurement post-processing (Apogee Instruments, 2020). The software is also able to convert measured CCI values to Konica Minolta SPAD-502+ units using a pre-defined conversion

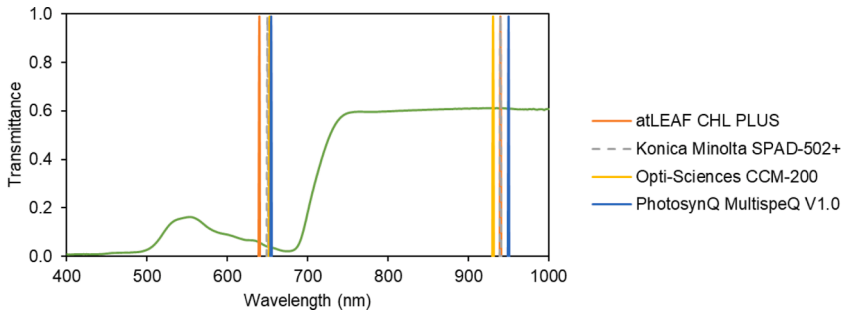

Fig. 1. Example transmittance spectrum of a hawthorn leaf sampled on 25/06/2021, in addition to the position of the central wavelengths of the bands used by each chlorophyll meter.

function (Apogee Instruments, 2020; Parry et al., 2014).

2.3. Chlorophyll meter and transmittance measurements

Prior to chlorophyll meter measurements, reference readings were carried out with the Konica Minolta SPAD-502+ and Opti-Sciences CCM-200 according to manufacturer instructions (i.e. with no sample in the measurement head). By contrast, the manufacturers of the atLEAF CHL PLUS and PhotosynQ MultispeQ V1.0 do not specify pre-measurement reference readings. To ensure all chlorophyll meter and transmittance measurements were obtained from the same approximate area, a 20 mm diameter circle was marked out on one side of each leaf, approximately one to two thirds of the way down from its tip, avoiding the mid-rib and any major veins. Within this circle, three readings were made with each chlorophyll meter, and the mean was computed. Note that unlike the other investigated chlorophyll meters, the atLEAF CHL PLUS does not clamp the leaf, meaning that ambient light and slight movements of the leaf might influence the measurement. To further assess these potential limitations, we analysed the variability of the replicate measurements taken with each chlorophyll meter by calculating the coefficient of variation for each sampled leaf (Appendix A).

Spectrally-resolved conical-hemispherical leaf transmittance was determined between 350 nm and 1050 nm using an Analytical Spectral Devices (ASD) FieldSpec 3 Visible Near-Infrared (VNIR) spectroradiometer coupled to a LI-COR 1800-12 integrating sphere. The spectroradiometer's radiometric and wavelength calibrations were verified against a reference radiance gauge and known emission peaks from a mercury-argon lamp at the National Physical Laboratory (NPL). Immediately before measuring each batch of 15 leaves, the integration time of the spectroradiometer was optimised with respect to the illumination conditions within the sphere. For each leaf, reference (i.e. light entering directly into the sphere) and sample (i.e. light passing through the leaf) spectra were recorded according to the sphere's manual, with transmittance calculated as the ratio of the latter to the former (LI-COR, 1988). As a consequence, absolute radiometric calibration was not a strict necessity (Origo et al., 2020). Within the 20 mm circle marked on each leaf, the mean of three transmittance spectra was recorded, with each measurement sequence taking approximately 30 s.

Once chlorophyll meter and transmittance measurements were complete, leaf thickness in the centre of the 20 mm circle was determined using a digital thickness gauge. To investigate the potential influence of leaf thickness on chlorophyll meter outputs, the non-parametric Spearman's rank correlation coefficient (r_s) was calculated, enabling the strength of any monotonic associations to be quantified (Appendix B). Leaves were then placed back into their sample bags and frozen until destructive LCC determination.

2.4. Destructive determination of leaf chlorophyll concentration

In the laboratory, LCC was determined spectrophotometrically following the protocol defined by Brown et al. (2021). From the centre of the 20 mm circle marked on each leaf, a disc was removed using a 6 mm diameter cork borer. Each disc was placed in a polypropylene tube filled with 5 ml of dimethyl-sulphoxide (DMSO), before being left overnight in a drying oven at 65 °C. Once each disc was white in colour (indicating that all chlorophyll had been extracted), a 3 ml aliquot of the solution was transferred to a 10 mm path length polystyrene cuvette with a transfer pipette. Using a ThermoFisher Genesys 50 UV-Vis spectrophotometer, the absorbance of each sample was measured at 649 nm and 665 nm. From Wellburn's (1994) equations for DMSO, the concentrations of chlorophyll-a and -b were then determined (in μg ml^{-1}) as

$$C_a = 12.19\ A_{665} - 3.45\ A_{649} \tag{3}$$

$$C_b = 21.99\ A_{649} - 5.32\ A_{665} \tag{4}$$

where A_{649} and A_{665} are the absorbance values provided by the spectrophotometer at 649 nm and 665 nm, respectively. Total LCC was calculated (in g m^{-2}) as

$$LCC = \frac{(C_a + C_b)\ V}{A} \tag{5}$$

where V and A are the volume of extraction solvent (in ml) and area of the leaf disc (in mm^2), respectively.

Although our measurements were determined on a mass per unit area basis, it is worth noting that conversion to molar density (i.e. mol m^{-2}), as often used by plant physiologists, is relatively straightforward. Chlorophyll-a and -b have a molar mass of 893.51 g mol^{-1} and 907.47 g mol^{-1}, respectively, and chlorophyll-a is typically between two to three times as abundant as chlorophyll-b. As such, a weighted average equates to 897.58 ± 0.58 g mol^{-1}, enabling the molar density to be approximated as

$$LCC\ (mol\ m^{-2}) \sim \frac{LCC\ (g\ m^{-2})}{897.58} \tag{6}$$

2.5. Calibration and characterisation of the chlorophyll meters

Calibration functions relating the values provided by each chlorophyll meter to destructively-determined LCC were established using non-linear least squares regression. For the atLEAF CHL PLUS, Konica Minolta SPAD-502+, and PhotosynQ MultispeQ V1.0, the calibration functions took an exponential form, whereas for the Opti-Sciences CCM-200, logarithmic calibration functions were adopted. In addition to overall (i.e. generic) calibration functions, individual calibration functions were established for each investigated species. To determine whether there were significant differences between the generic and species-specific calibration functions, we computed prediction uncertainties for each species-specific calibration function and compared them to LCC values provided by the generic calibration function when applied to that species (Appendix C). To assess how the choice of calibration function affected the accuracy of derived LCC estimates, we applied the generic and species-specific calibration functions to the chlorophyll meter outputs for each species, comparing the results with the destructively-determined values by means of the root mean square error (RMSE) and normalised RMSE. The NRMSE was computed by dividing the RMSE by the range of destructively determined values (Appendix C).

In addition to relationships with destructively-determined LCC, the relationships between the different chlorophyll meters were also characterised, enabling conversion functions between chlorophyll meter outputs to be derived. Specifically, linear functions were established to relate the outputs of the atLEAF CHL PLUS, Konica Minolta SPAD-502+, and PhotosynQ MultispeQ V1.0 to each other, whilst logarithmic (and exponential) functions were used to relate the Opti-Sciences CCM-200 outputs to the outputs of the other chlorophyll meters (and vice versa). Finally, we compared our calibration and conversion functions with those detailed in previously published work (Appendix D).

2.6. Assessment of transmittance spectroscopy

From the transmittance measurements performed with the spectroradiometer and integrating sphere, four indices using the same wavelengths and measurement equations as each of the chlorophyll meters were calculated (excluding the k and C coefficients in Eq. (1), which are undisclosed by the instrument manufacturers). Given the potentially higher quality, signal-to-noise, and sensitivity characteristics of the spectroradiometer, we hypothesised that these indices would be characterised by stronger relationships with destructively-determined LCC than the chlorophyll meter outputs. Calibration functions relating the transmittance-based indices to destructively-determined LCC were established as described in Section 2.5, enabling their performance to be

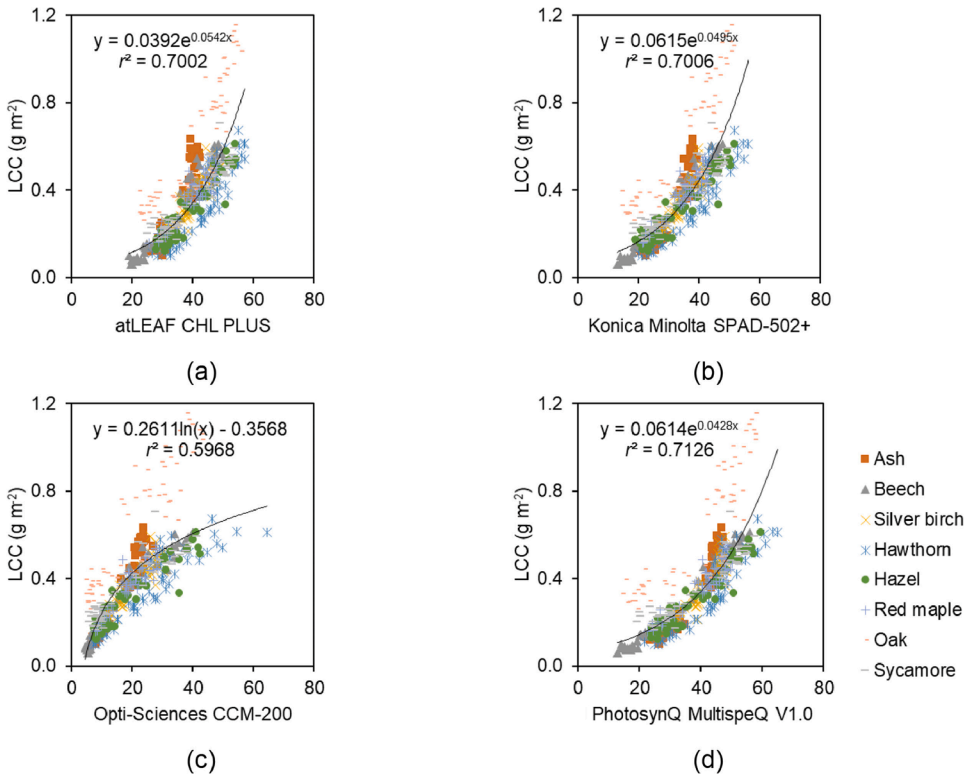

Fig. 2. Overall relationships between the outputs of the atLEAF CHL PLUS (a), Konica Minolta SPAD-502+ (b), Opti-Sciences CCM-200 (c), and PhotosynQ MultispeQ V1.0 (d) and destructively-determined LCC, for all investigated species.

Table 3
Relationships between the outputs of each chlorophyll meter and destructively-determined LCC, per species. The minimum and maximum chlorophyll meter and LCC values associated with each calibration function are detailed in Appendix C.

Species	atLEAF CHL PLUS Calibration function	r^2	RMSE (g m^{-2})	Konica Minolta SPAD-502+ Calibration function	r^2	RMSE (g m^{-2})	Opti-Sciences CCM-200 Calibration function	r^2	RMSE (g m^{-2})	PhotosynQ MultispeQ V1.0 Calibration function	r^2	RMSE (g m^{-2})
Ash	$y = 0.009e^{0.098x}$	0.88	0.07	$y = 0.0179e^{0.0884x}$	0.94	0.05	$y = 0.3713\ln(x) - 0.6656$	0.90	0.05	$y = 0.0211e^{0.0696x}$	0.95	0.05
Beech	$y = 0.0198e^{0.0723x}$	0.95	0.06	$y = 0.0344e^{0.065x}$	0.94	0.06	$y = 0.2515\ln(x) - 0.3473$	0.97	0.03	$y = 0.0391e^{0.053x}$	0.96	0.04
Silver birch	$y = 0.0442e^{0.0513x}$	0.83	0.05	$y = 0.0565e^{0.0519x}$	0.86	0.05	$y = 0.2905\ln(x) - 0.4907$	0.86	0.04	$y = 0.0471e^{0.0488x}$	0.87	0.04
Hawthorn	$y = 0.0174e^{0.065x}$	0.87	0.08	$y = 0.0344e^{0.0564x}$	0.90	0.08	$y = 0.2718\ln(x) - 0.4901$	0.86	0.06	$y = 0.0336e^{0.0504x}$	0.87	0.09
Hazel	$y = 0.0366e^{0.0519x}$	0.85	0.05	$y = 0.0641e^{0.0441x}$	0.86	0.04	$y = 0.2368\ln(x) - 0.3552$	0.89	0.04	$y = 0.0598e^{0.04x}$	0.89	0.04
Red maple	$y = 0.047e^{0.0504x}$	0.86	0.05	$y = 0.0676e^{0.0479x}$	0.87	0.05	$y = 0.2644\ln(x) - 0.398$	0.86	0.04	$y = 0.0693e^{0.0401x}$	0.88	0.04
Oak	$y = 0.117e^{0.0397x}$	0.87	0.10	$y = 0.1719e^{0.0355x}$	0.87	0.11	$y = 0.3355\ln(x) - 0.286$	0.82	0.12	$y = 0.1785e^{0.0303x}$	0.85	0.11
Sycamore	$y = 0.0648e^{0.0407x}$	0.87	0.05	$y = 0.0951e^{0.037x}$	0.88	0.05	$y = 0.2151\ln(x) - 0.2348$	0.86	0.05	$y = 0.0956e^{0.032x}$	0.88	0.05
All	$y = 0.0392e^{0.0542x}$	0.70	0.12	$y = 0.0615e^{0.0495x}$	0.70	0.12	$y = 0.2611\ln(x) - 0.3568$	0.60	0.13	$y = 0.0614e^{0.0428x}$	0.71	0.12
All excl. oak	$y = 0.0338e^{0.0561x}$	0.79	0.09	$y = 0.0516e^{0.0524x}$	0.81	0.08	$y = 0.2477\ln(x) - 0.3588$	0.84	0.06	$y = 0.0501e^{0.046x}$	0.85	0.07

directly compared with the chlorophyll meters themselves. By regressing the indices against the corresponding chlorophyll meter outputs, we could also estimate the *k* and *C* coefficients as the slope and intercept of the linear regression equation. We further investigated whether a different choice of wavelengths could provide improved relationships with destructively-determined LCC. To do this, we tested all possible combinations of wavelengths, excluding those below 400 nm and above 1000 nm to avoid noise at the limits of the wavelength range of the spectroradiometer (Burnett et al., 2021).

To take advantage of the substantially increased spectral sampling offered by the transmittance measurements (which remains unexploited when using simple two-band indices as adopted by the chlorophyll meters), a full-spectrum approach to estimating LCC was also evaluated. This involved establishing partial least squares regression (PLSR) models relating transmittance spectra to destructively-determined LCC. PLSR is a technique, originally developed in the field of chemometrics, for use with datasets subject to a high degree of collinearity (as is the case with spectral datasets, whose adjacent bands are highly correlated). The

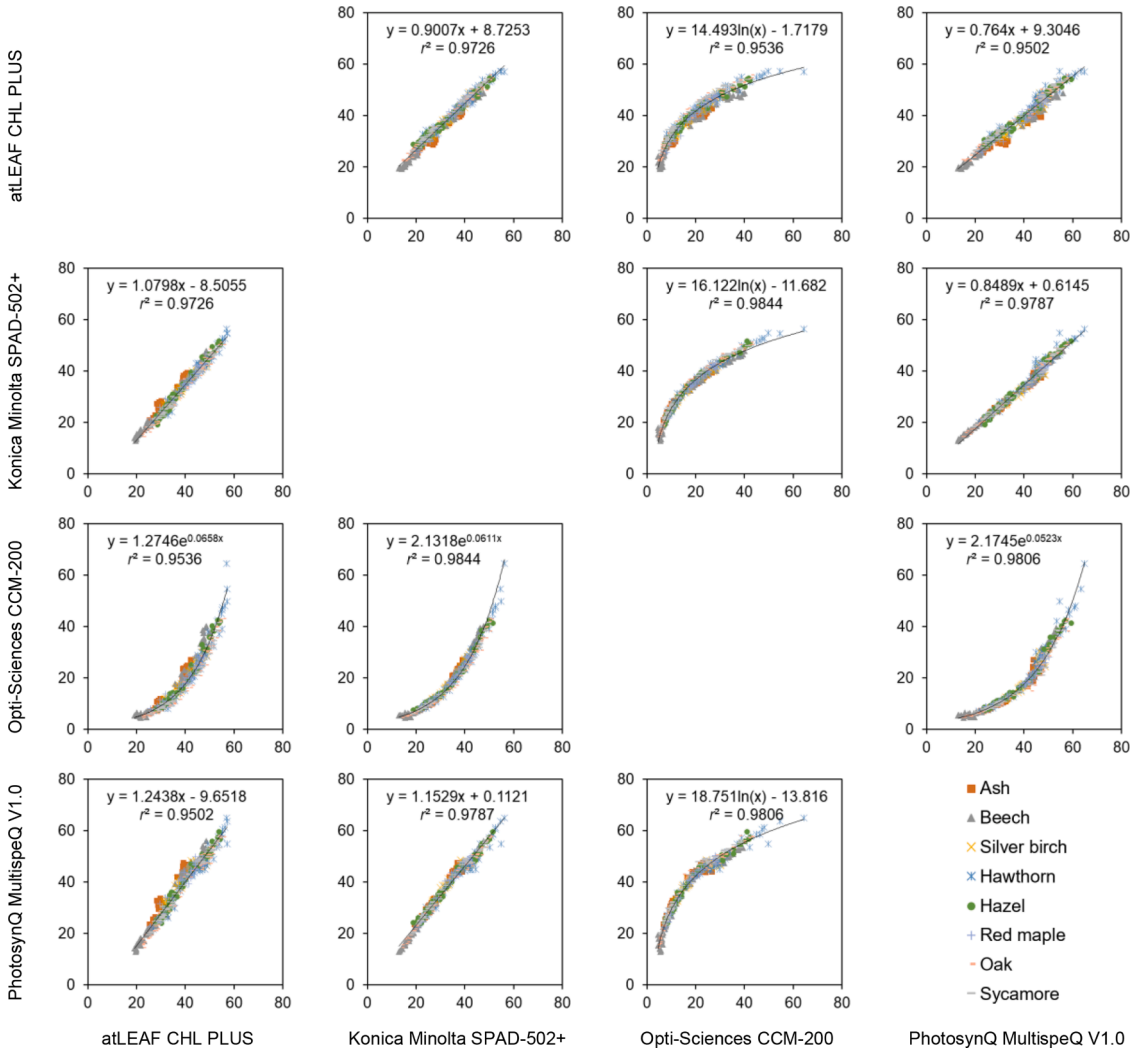

Fig. 3. Relationships between the outputs of each chlorophyll meter.

approach is widely used to relate biophysical and biochemical variables to remotely-sensed multispectral and hyperspectral imagery (Atzberger et al., 2010; Darvishzadeh et al., 2011; Herrmann et al., 2011; Sakowska et al., 2016; Upreti et al., 2019; Wang et al., 2020), as well as field spectroscopy data (Asner et al., 2011; Chavana-Bryant et al., 2017; Féret et al., 2011; Hill et al., 2019). It involves the transformation of inputs into a set of uncorrelated components using principle components analysis (PCA), with regression performed on the resulting PCA scores (Atzberger et al., 2010; Burnett et al., 2021; Hansen and Schjoerring, 2003). Again, wavelengths below 400 nm and above 1000 nm were excluded from the analysis (Burnett et al., 2021).

3. Results

3.1. Relationships between chlorophyll meter outputs and leaf chlorophyll concentration

The outputs of the atLEAF CHL PLUS, Konica Minolta SPAD-502+, and PhotosynQ MultispeQ V1.0 all demonstrated strong exponential relationships with destructively-determined LCC, with the overall calibration functions (which covered all species) yielding coefficient of determination (r^2) values of 0.70 to 0.71 and a root mean square error (RMSE) of 0.12 g m^{-2} (Fig. 2 and Table 3). A weaker overall relationship with destructively-determined LCC was demonstrated by the Opti-Sciences CCM-200, whose logarithmic calibration function was characterised by an r^2 of 0.60 and RMSE of 0.13 g m^{-2} (Fig. 2c and Table 3). Regardless of the chlorophyll meter in question, with the exception of oak, relatively consistent relationships were demonstrated for all species (Fig. 2). Indeed, when oak samples were excluded from the derivation of overall calibration functions, r^2 values rose to between 0.79 and 0.85 (RMSE = 0.06 g m^{-2} to 0.09 g m^{-2}), with the greatest increase observed in the case of the Opti-Sciences CCM-200 (r^2 = 0.84, RMSE = 0.06 g m^{-2}) (Table 3). Some further improvements in r^2 and RMSE were achieved when individual calibration functions were established for each species (r^2 = 0.82 to 0.97, RMSE = 0.03 g m^{-2} to 0.12 g m^{-2}) (Table 3).

3.2. Comparison between generic and species-specific calibration functions

In the majority of cases, LCC values provided by the generic calibration functions (derived using all samples excluding oak) fell within the prediction uncertainties of the associated species-specific calibration functions over the range of sampled values (Appendix C). Exceptions were hawthorn and hazel, where for all instruments except the Opti-Sciences CCM-200, LCC values provided by the generic calibration functions slightly exceeded the prediction uncertainties towards the higher range of sampled values (i.e. LCC > 0.6 g m^{-2}). For oak, LCC values provided by the generic calibration functions exceeded the prediction uncertainties of the species-specific calibration functions for

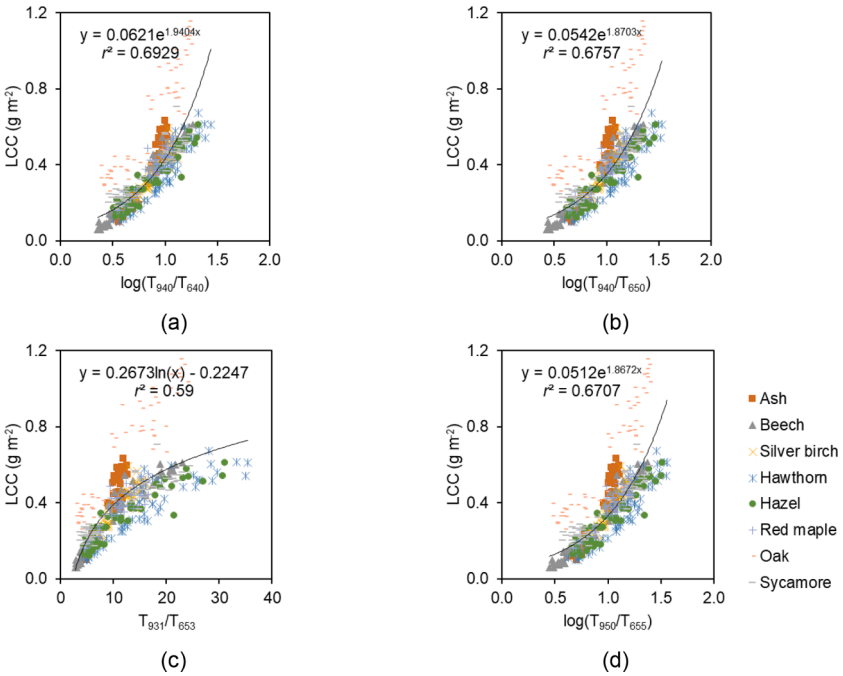

Fig. 4. Overall relationships between transmittance-based indices representing the wavelengths and measurement equations of the atLEAF CHL PLUS (a), Konica Minolta SPAD-502+ (b), Opti-Sciences CCM-200 (c), and PhotosynQ MultispeQ V1.0 (d) and destructively-determined LCC, for all investigated species.

Table 4
Relationships between each of the transmittance-based indices and destructively-determined LCC, per species.

Species	$\log(T_{940}/T_{640})$ Calibration function	r^2	RMSE (g m^{-2})	$\log(T_{940}/T_{650})$ Calibration function	r^2	RMSE (g m^{-2})	T_{931}/T_{653} Calibration function	r^2	RMSE (g m^{-2})	$\log(T_{950}/T_{655})$ Calibration function	r^2	RMSE (g m^{-2})
Ash	$y = 0.0215e^{3.2342x}$	0.95	0.05	$y = 0.0135e^{3.4825x}$	0.95	0.05	$y = 0.4426\ln(x) - 0.5746$	0.90	0.06	$y = 0.0111e^{3.6004x}$	0.94	0.05
Beech	$y = 0.0355e^{2.4356x}$	0.93	0.07	$y = 0.0281e^{2.4403x}$	0.94	0.06	$y = 0.2693\ln(x) - 0.2455$	0.97	0.03	$y = 0.0256e^{2.4655x}$	0.94	0.06
Silver birch	$y = 0.0552e^{2.032x}$	0.89	0.04	$y = 0.0468e^{2.0285x}$	0.89	0.04	$y = 0.3047\ln(x) - 0.3408$	0.86	0.04	$y = 0.0433e^{2.0525x}$	0.88	0.04
Hawthorn	$y = 0.0354e^{2.2158x}$	0.91	0.08	$y = 0.0293e^{2.1452x}$	0.90	0.08	$y = 0.2688\ln(x) - 0.3399$	0.85	0.06	$y = 0.0274e^{2.1379x}$	0.89	0.08
Hazel	$y = 0.0641e^{1.7404x}$	0.87	0.04	$y = 0.0541e^{1.6852x}$	0.87	0.04	$y = 0.226\ln(x) - 0.2106$	0.90	0.04	$y = 0.0505e^{1.6869x}$	0.86	0.05
Red maple	$y = 0.062e^{1.9876x}$	0.89	0.04	$y = 0.0539e^{1.8948x}$	0.87	0.05	$y = 0.2604\ln(x) - 0.2357$	0.84	0.04	$y = 0.0512e^{1.8888x}$	0.86	0.05
Oak	$y = 0.1691e^{1.4601x}$	0.88	0.10	$y = 0.1543e^{1.3933x}$	0.87	0.11	$y = 0.3557\ln(x) - 0.1531$	0.82	0.12	$y = 0.1468e^{1.3937x}$	0.87	0.11
Sycamore	$y = 0.0966e^{1.4644x}$	0.88	0.05	$y = 0.0857e^{1.4192x}$	0.88	0.05	$y = 0.2148\ln(x) - 0.1223$	0.87	0.05	$y = 0.0823e^{1.4122x}$	0.88	0.05
All	$y = 0.0621e^{1.9404x}$	0.69	0.13	$y = 0.0542e^{1.8703x}$	0.68	0.13	$y = 0.2673\ln(x) - 0.2247$	0.59	0.13	$y = 0.0512e^{1.8672x}$	0.67	0.13
All excl. oak	$y = 0.0513e^{2.066x}$	0.83	0.08	$y = 0.0441e^{1.9967x}$	0.81	0.08	$y = 0.2479\ln(x) - 0.2198$	0.81	0.07	$y = 0.0419e^{1.9873x}$	0.80	0.09

almost all sampled values (Appendix C), confirming that oak demonstrated a unique chlorophyll meter – LCC relationship when compared to the other investigated species. Over the species other than oak, use of the generic calibration functions as opposed to a species-specific one led to a mean increase in RMSE (NRMSE) of between 0.01 g m^{-2} and 0.02 g m^{-2} (2% and 5 %) and a maximum increase in RMSE (NRMSE) of between 0.03 g m^{-2} and 0.06 g m^{-2} (5% and 11%) depending on the instrument in question (Appendix C).

3.3. Relationships between the different chlorophyll meters

Strong linear relationships were demonstrated between the outputs of the atLEAF CHL PLUS, Konica Minolta SPAD-502+, and PhotosynQ MultispeQ V1.0 (r^2 = 0.95 to 0.98). In contrast, the outputs of the Opti-Sciences CCM-200 were characterised by logarithmic relationships with the outputs of the other chlorophyll meters (r^2 = 0.95 to 0.98). For all combinations, minimal scatter was observed (Fig. 3). It is worth noting that a small but distinct step in the outputs of the PhotosynQ MultispeQ V1.0 was observed, occurring at values of greater than 50, whilst such a step was not apparent in the outputs of the atLEAF CHL PLUS, Konica Minolta SPAD-502+, or Opti-Sciences CCM-200 (Fig. 3). Despite the fact that the atLEAF CHL PLUS does not clamp the leaf, its measurements were no more variable than those of the other investigated chlorophyll meters (Appendix A).

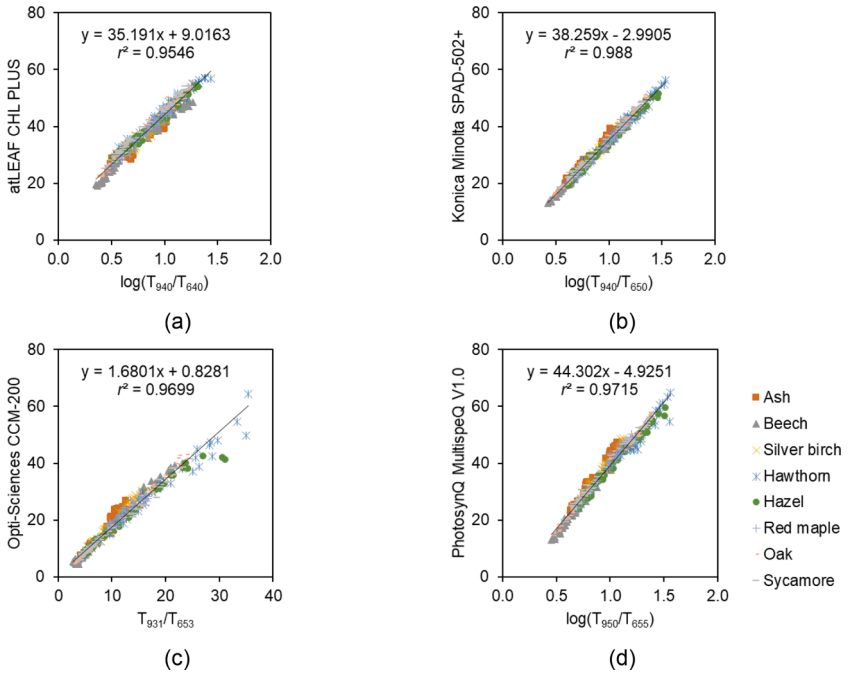

Fig. 5. Relationships between chlorophyll meter output values and transmittance-based indices representing the wavelengths and measurement equations of the atLEAF CHL PLUS (a), Konica Minolta SPAD-502+ (b), Opti-Sciences CCM-200 (c), and PhotosynQ MultispeQ V1.0 (d).

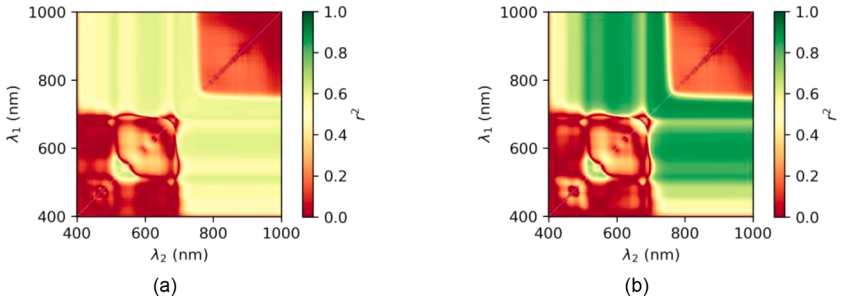

Fig. 6. Variation in r^2 of relationships between the transmittance-based index $\log(T_{\lambda 1}/T_{\lambda 2})$ and destructively-determined LCC, as a function of incorporated wavelengths, for all species (a), and all species excluding oak (b).

3.4. Relationships between transmittance-based indices and leaf chlorophyll concentration

When compared with the outputs of the chlorophyll meters themselves, the transmittance-based indices calculated using the associated wavelengths and measurement equations demonstrated very similar relationships with destructively-determined LCC, albeit with slightly reduced r^2 and slightly increased RMSE values (Fig. 4 and Table 4). As expected, the $\log(T_{940}/T_{640})$, $\log(T_{940}/T_{650})$, and $\log(T_{950}/T_{655})$ indices based on the atLEAF CHL PLUS, Konica Minolta SPAD-502+, and PhotosynQ MultispeQ V1.0 demonstrated exponential relationships with destructively-determined LCC ($r^2 = 0.67$ to 0.69, RMSE = 0.13 g m^{-2}), whilst the T_{931}/T_{653} index based on the Opti-Sciences CCM-200 demonstrated a logarithmic relationship ($r^2 = 0.59$, RMSE = 0.13 g m^{-2}) (Fig. 4 and Table 4). Once again, increases in r^2 and RMSE were achieved for overall calibration functions excluding oak samples (r^2 = 0.80 to 0.83, RMSE = 0.07 g m^{-2} to 0.09 g m^{-2}), and for individual calibration functions established for each species ($r^2 = 0.82$ to 0.97, RMSE = 0.03 g m^{-2} to 0.12 g m^{-2}) (Table 4).

3.5. Relationships between transmittance-based indices and corresponding chlorophyll meter outputs

All of the transmittance-based indices demonstrated strong linear relationships with the outputs of the chlorophyll meters upon which they were based ($r^2 = 0.95$ to 0.99). For the atLEAF CHL PLUS, the *k* and *C* coefficients were estimated as approximately 35.19 and 9.02, respectively, whilst values of approximately 38.26 and -2.99 were estimated for the Konica Minolta SPAD-502+ (Fig. 5). Values of approximately 44.30 and -4.93 were estimated for the PhotosynQ MultispeQ V1.0, whilst values of approximately 1.68 and 0.83 were estimated for the Opti-Sciences CCM-200 (Fig. 5).

3.6. Relationships between transmittance-based indices and leaf chlorophyll concentration as a function of incorporated wavelengths

When relationships between the transmittance-based index $\log(T_{\lambda 1}/T_{\lambda 2})$ and destructively-determined LCC were assessed using all possible combinations of wavelengths, the results demonstrated that reasonably strong relationships could be obtained provided that λ_1 was located in the near-infrared region (between 700 nm and 1000 nm) and λ_2 was located in the visible region (between 400 and 700 nm) or vice versa. When all species were considered, the highest r^2 value was achieved

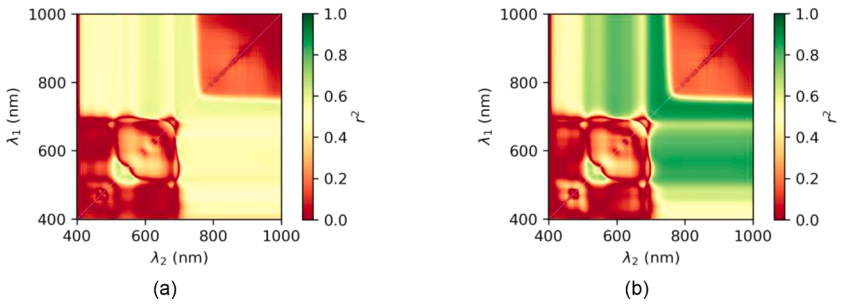

Fig. 7. Variation in r^2 of relationships between the transmittance-based index $T_{\lambda1}/T_{\lambda2}$ and destructively-determined LCC, as a function of incorporated wavelengths, for all species (a), and all species excluding oak (b).

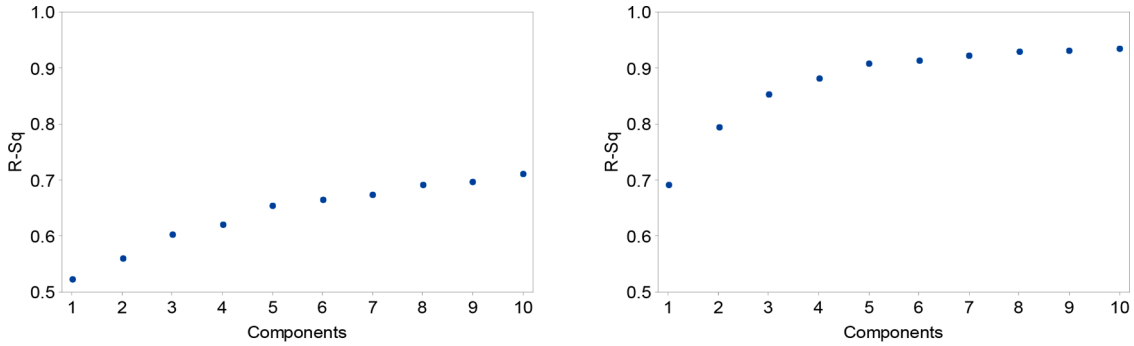

Fig. 8. Variation in r^2 of PLSR models relating transmittance spectra to destructively-determined LCC as a function of the number of components incorporated in the model for all species (a), and all species excluding oak (b).

Table 5
Performance of PLSR models relating transmittance spectra to destructively-determined LCC (established using 10 components), per species.

Species	r^2	RMSE (g m^{-2})
Ash	0.99	0.02
Beech	1.00	0.02
Silver birch	0.98	0.02
Hawthorn	0.99	0.02
Hazel	0.97	0.03
Red maple	0.99	0.01
Oak	0.98	0.05
Sycamore	0.98	0.02
All	0.71	0.11
All excl. oak	0.93	0.04

when $\lambda_1 = 842$ nm and $\lambda_2 = 521$ nm ($r^2 = 0.81$) (Fig. 6a). When oak was excluded, stronger relationships were obtained overall (Fig. 6b). In contrast to the dataset including all species, in this case, the best performing combination of wavelengths was found in the green region ($\lambda_1 = 558$ nm and $\lambda_2 = 521$ nm, $r^2 = 0.90$), offering some improvement over the chlorophyll meters (and transmittance-based indices based on their measurement equations and wavelengths). Almost identical results were obtained for the transmittance-based index $T_{\lambda1}/T_{\lambda2}$ (Fig. 7).

3.7. Partial least squares regression models relating transmittance spectra to leaf chlorophyll concentration

When compared to the investigated chlorophyll meters and transmittance-based indices, the full-spectrum approach using PLSR demonstrated improved r^2 and RMSE values in the majority of cases. All PLSR models were established using 10 components, as fewer

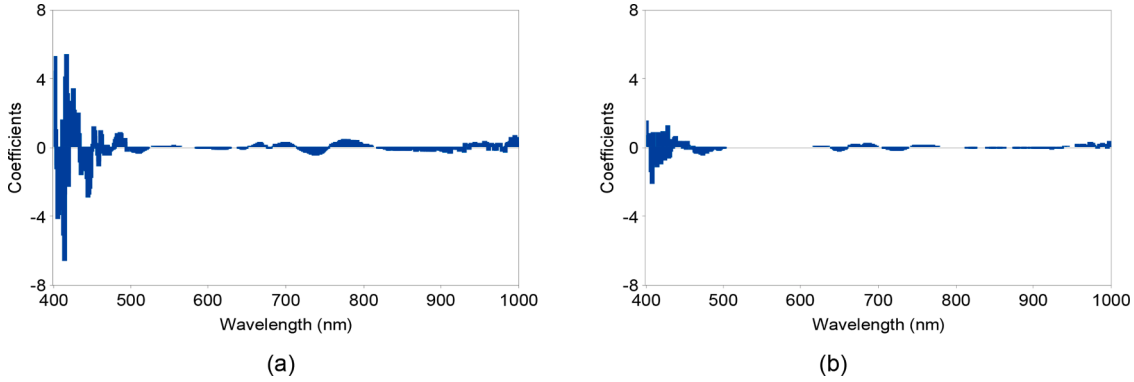

Fig.9. Coefficients associated with each wavelength for PLSR models relating transmittance spectra to destructively-determined LCC (established using 10 components), for all species (a), and all species excluding oak (b).

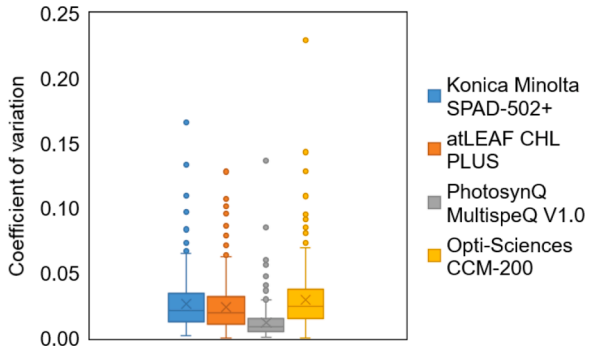

Fig. A1. Box plots of the coefficient of variation of replicate chlorophyll meter measurements made on each leaf.

Table B1
Spearman's rank correlation between the outputs of each chlorophyll meter and leaf thickness. Cases with a significant correlation ($p < 0.05$) are indicated with *.

Species	atLEAF CHL PLUS	Konica Minolta SPAD-502+	Opti-Sciences CCM-200	PhotosynQ MultispeQ V1.0
Ash	-0.39*	-0.48*	-0.54*	-0.56*
Beech	0.10	0.14	0.12	0.13
Silver birch	-0.49*	-0.55*	-0.55*	-0.56*
Hawthorn	-0.40*	-0.37*	-0.38*	-0.39*
Hazel	-0.34*	-0.32*	-0.31*	-0.32*
Red maple	0.40*	0.36*	0.36*	0.32*
Oak	-0.17	-0.15	-0.18	-0.15
Sycamore	-0.39*	-0.40*	-0.43*	-0.40*
All	-0.06	-0.06	-0.10*	-0.08
All excl. oak	-0.06	-0.05	-0.09	-0.08

components led to reductions in r^2 (Fig. 8). For the overall PLSR model covering all species, r^2 and RMSE values were similar to the chlorophyll meters and transmittance-based indices ($r^2 = 0.71$, RMSE = 0.11 g m^{-2}), but markedly greater than these methods when a) oak samples were excluded ($r^2 = 0.93$, RMSE = 0.04 g m^{-2}), and b) in the case of individual PLSR models established for each species ($r^2 = 0.97$ to 1.00, RMSE = 0.01 g m^{-2} to 0.05 g m^{-2}) (Table 5). A useful feature of PLSR is that the relative importance of each input variable can be assessed by examining the associated coefficients, enabling the most informative spectral bands to be determined. The largest coefficients were observed at visible wavelengths between 400 nm and 500 nm, whilst noticeable peaks were also observed in the red and near-infrared regions, at wavelengths between 600 nm and 800 nm and 900 nm to 1000 nm (Fig. 9).

4. Discussion

4.1. Performance of the investigated chlorophyll meters

Whilst a range of chlorophyll meters are now available, few comprehensive assessments of performance involving multiple models have been conducted, particularly in the case of forest environments (Cahyo et al., 2020; Cerovic et al., 2012; Dong et al., 2019; Mendoza-Tafolla et al., 2019; Parry et al., 2014; Richardson et al., 2002; Zhu et al., 2012). We assessed the relationships between the outputs of four chlorophyll meters and destructively-determined LCC for eight deciduous broadleaf forest species, using the same leaf samples to ensure a fair comparison. Our results demonstrated similarly strong relationships with destructively-determined LCC for all chlorophyll meters, indicating that once calibrated, any of the investigated models represent a suitable choice for non-destructive forest LCC estimation. Notably, our results revealed that even low-cost chlorophyll meters such as the atLEAF CHL PLUS and PhotosynQ MultispeQ V1.0 can provide similar (and in some cases, stronger) relationships with destructively-determined LCC when compared with well-established instruments such as the Konica Minolta SPAD-502+ and Opti-Sciences CCM-200. In the case of the atLEAF CHL PLUS, this is despite the fact that the instrument does not clamp the leaf (which could allow the ingress of ambient light and slight movements of the leaf). Similar results were presented by Zhu et al. (2012), who found atLEAF CHL PLUS measurements demonstrated no significant effects associated with irradiance or time of day.

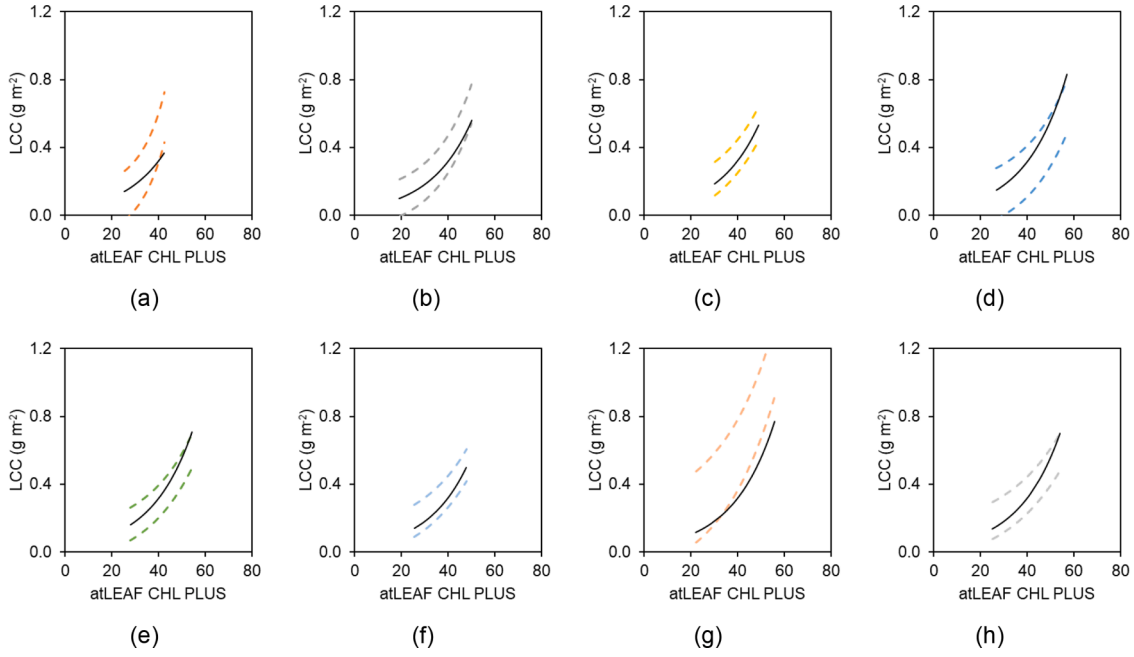

Fig. C1. Comparison of the generic atLEAF CHL PLUS calibration function derived using all samples excluding oak (solid black line) against the 95% prediction intervals (dashed lines) associated with species-specific calibration functions for ash (a), beech (b), silver birch (c), hawthorn (d), hazel (e), red maple (f), oak (g), and sycamore (h).

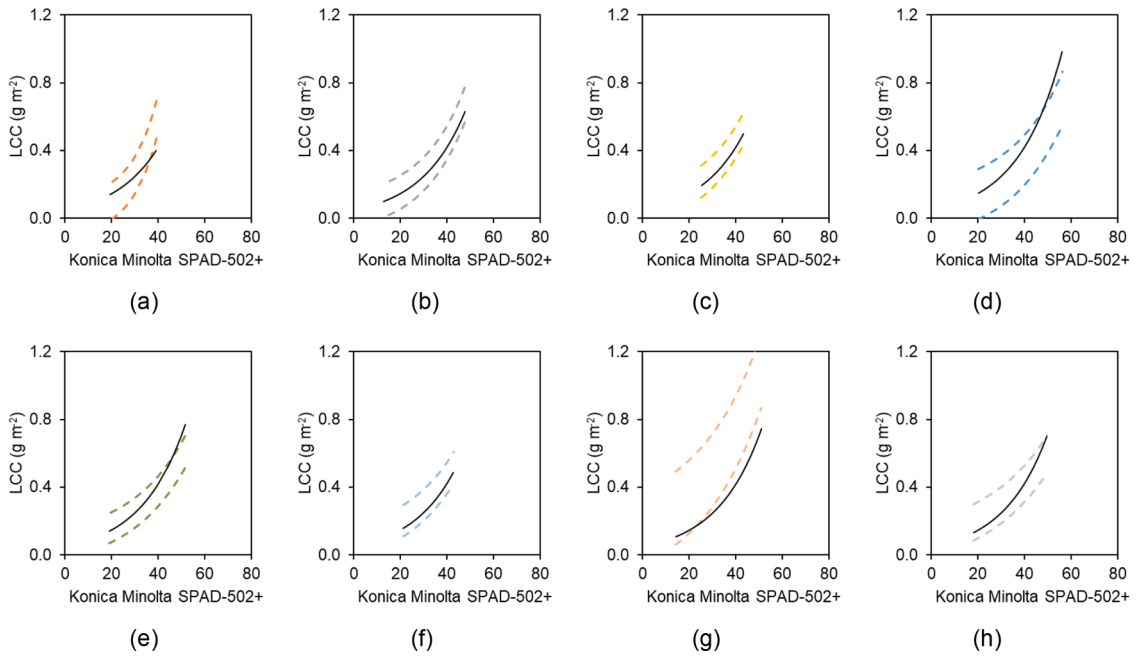

Fig. C2. Comparison of the generic Konica Minolta SPAD-502+ calibration function derived using all samples excluding oak (solid black line) against the 95% prediction intervals (dashed lines) associated with species-specific calibration functions for ash (a), beech (b), silver birch (c), hawthorn (d), hazel (e), red maple (f), oak (g), and sycamore (h).

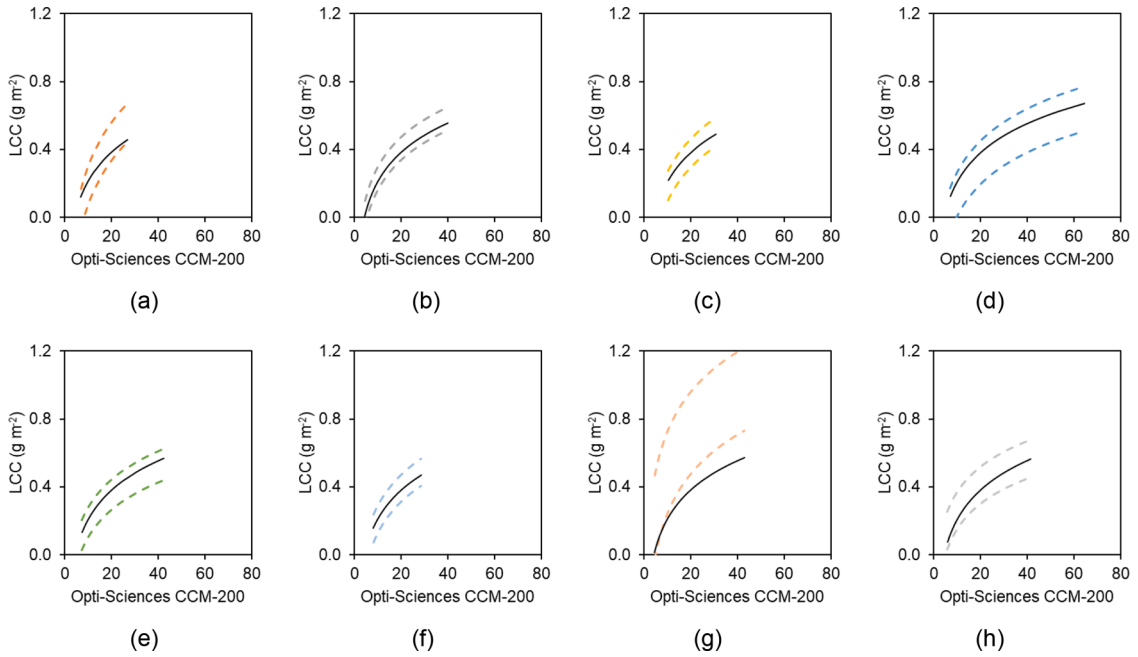

Fig. C3. Comparison of the generic Opti-Sciences CCM-200 calibration function derived using all samples excluding oak (solid black line) against the 95% prediction intervals (dashed lines) associated with species-specific calibration functions for ash (a), beech (b), silver birch (c), hawthorn (d), hazel (e), red maple (f), oak (g), and sycamore (h).

In addition to their core measurement capabilities, it is worth noting that the latest versions of the Opti-Sciences CCM-200 (and the Apogee Instruments MC-100 derivative) incorporate integrated global positioning system (GPS) functionality (ADC Bioscientific, 2019; Apogee Instruments, 2020), whilst the PhotosynQ MultispeQ V1.0 is operated via a smartphone application, enabling measurements to be geotagged and uploaded to the cloud. Using other sensors on the PhotosynQ MultispeQ V1.0, variables such as ambient temperature, humidity, leaf angle, leaf temperature, and incoming photosynthetically active radiation (PAR) can also be automatically recorded, in addition to a range of fluorescence base parameters (PhotosynQ, 2021a). For certain applications, these features could result in substantial labour savings in the field. As manufactured, the Konica Minolta SPAD-502+ does not allow storage of measurements (Konica Minolta, 2009), though a modified version incorporates a data logger, as well as geotagging functionality if connected to a compatible GPS unit (Spectrum Technologies, 2009). Whilst the atLEAF CHL PLUS does contain a data logger, it does not provide GPS functionality (FT Green, 2018).

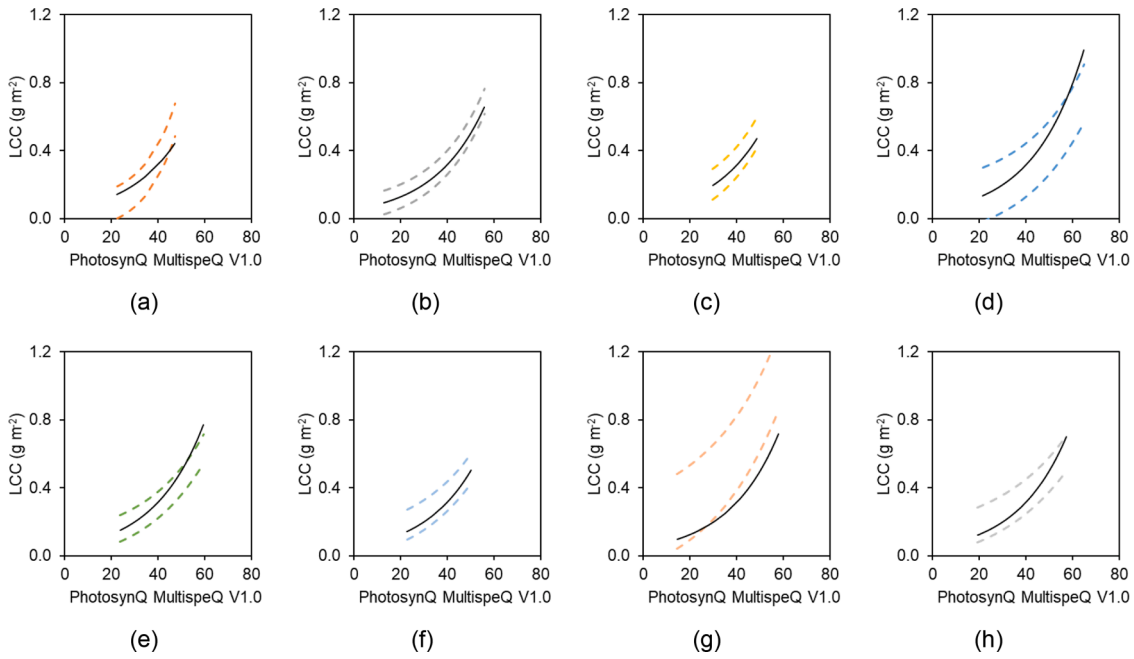

Fig. C4. Comparison of the generic PhotosynQ MultispeQ V1.0 calibration function derived using all samples excluding oak (solid black line) against the 95% prediction intervals (dashed lines) associated with species-specific calibration functions for ash (a), beech (b), silver birch (c), hawthorn (d), hazel (e), red maple (f), oak (g), and sycamore (h).

Table C1
Minimum and maximum chlorophyll meter and destructively-determined LCC values associated with each calibration function.

	atLEAF CHL PLUS		Konica Minolta SPAD-502+		Opti-Sciences CCM-200		PhotosynQ MultispeQ V1.0		LCC (g m^{-2})	
	Minimum	Maximum	Minimum	Maximum	Minimum	Maximum	Minimum	Maximum	Minimum	Maximum
Ash	25.40	42.43	19.43	39.17	6.93	26.80	22.40	47.26	0.10	0.63
Beech	19.13	50.10	12.90	47.70	4.43	40.00	12.90	55.91	0.06	0.61
Silver birch	30.23	49.07	25.33	43.20	10.33	30.60	29.72	48.72	0.19	0.59
Hawthorn	26.70	57.10	20.17	56.23	7.07	64.40	21.53	64.91	0.10	0.67
Hazel	28.00	54.27	18.97	51.57	7.33	42.33	23.78	59.46	0.12	0.61
Red maple	25.57	47.90	21.30	42.83	8.07	28.50	22.76	50.12	0.16	0.55
Oak	22.20	55.73	14.27	51.00	4.53	42.90	14.46	57.86	0.26	1.16
Sycamore	25.13	54.03	18.10	49.70	5.80	41.40	19.35	57.41	0.17	0.70
All	19.13	57.10	12.90	56.23	4.43	64.40	12.90	64.91	0.06	1.16
All excl. oak	19.13	57.10	12.90	56.23	4.43	64.40	12.90	64.91	0.06	0.70

4.2. Species-specificity of the chlorophyll meter – leaf chlorophyll concentration relationship and the influence of environmental conditions

With the exception of oak, relationships between chlorophyll meter outputs and destructively-determined LCC were consistent for all investigated species, despite previous work that has suggested that species-specific calibration functions are a necessity for accurate LCC estimation (Dash et al., 2010; Demarez et al., 1999; Dong et al., 2019; Percival et al., 2008; Uddling et al., 2007). Although species-specific calibration functions provided the most accurate LCC estimates, our results imply that for these seven temperate deciduous broadleaf forest species, generic rather than species-specific calibration functions may be suitable for many users, provided that a small reduction in accuracy is acceptable for the application at hand. Excluding oak, the generic calibration functions were able to explain between 2% and 16% less variation in LCC than the species-specific calibration functions, resulting in a mean increase in RMSE (NRMSE) of just 0.01 g m^{-2} to 0.02 g m^{-2} (2% to 5%). Meanwhile, LCC values provided by the generic calibration functions fell within the prediction uncertainties of the species-specific calibration functions for most considered species. It is worth noting that similar conclusions were drawn by Coste et al. (2010), Cerovic et al. (2012), and Parry et al. (2014) for other species. Indeed, for tropical rainforest species, Coste et al. (2010) argue that the practicality of a generic calibration function 'clearly outweighs limitations due to the slight loss of model accuracy'.

It should be stressed that these results apply only to the investigated temperate deciduous broadleaf forest species (and over the range of LCC values observed in our study – see Appendix A). Indeed, previous work suggests that a generic calibration function for such species would not accurately predict LCC if applied to distinctly different species such as crops (Parry et al., 2014). Future work should consider a wider range of species and LCC values, including leaves from species characterised by high LCC such as ivy (*Hedera helix*) and holly (*Ilex aquifolium),* in addition to chlorotic leaves with low LCC. For oak, we hypothesise that relationships between chlorophyll meter outputs and destructively-determined LCC lacked consistency with the other species due to a less uniform distribution of chlorophyll at the leaf level, leading to increased sieve and detour effects (Cerovic et al., 2012; Markwell et al., 1995; Monje and Bugbee, 1992; Nauš et al., 2010; Parry et al., 2014; Uddling et al., 2007). Further experiments, which were beyond the scope of the present study, will be required to test this hypothesis.

If pre-defined calibration functions are to be adopted by chlorophyll meter users, an important question is whether environmental conditions (such as soil fertility and sunlight received) may influence the chlorophyll meter – LCC relationship. In previous work, Parry et al. (2014) suggested that environmental conditions had no significant effect,

Table C2
RMSE and NRMSE values associated with generic and species-specific calibration functions when evaluated against destructively-determined LCC.

Instrument	Species	RMSE (g m^{-2})			NRMSE (%)		
		Generic	Specific	Difference	Generic	Specific	Difference
atLEAF CHL PLUS	Ash	0.13	0.07	0.06	24.51	13.19	11.32
	Beech	0.07	0.06	0.01	12.52	11.53	0.99
	Silver birch	0.05	0.05	0.01	13.62	11.86	1.77
	Hawthorn	0.12	0.08	0.05	21.71	13.81	7.90
	Hazel	0.06	0.05	0.01	12.66	9.64	3.02
	Red maple	0.06	0.05	0.01	14.53	11.58	2.95
	Sycamore	0.08	0.05	0.02	13.90	9.87	4.03
	Mean	0.08	0.06	0.02	16.21	11.64	4.57
Konica Minolta SPAD-502+	Ash	0.11	0.05	0.05	20.00	9.96	10.04
	Beech	0.05	0.06	-0.01	9.44	11.11	-1.67
	Silver birch	0.05	0.05	0.01	13.10	11.19	1.92
	Hawthorn	0.13	0.08	0.05	23.04	14.21	8.84
	Hazel	0.07	0.04	0.02	13.83	8.90	4.93
	Red maple	0.06	0.05	0.02	15.28	11.49	3.79
	Sycamore	0.08	0.05	0.02	14.03	9.65	4.38
	Mean	0.08	0.05	0.02	15.53	10.93	4.60
Opti-Sciences CCM-200	Ash	0.08	0.05	0.03	15.23	10.27	4.95
	Beech	0.04	0.03	0.01	7.15	6.02	1.13
	Silver birch	0.04	0.04	0.00	10.82	10.05	0.77
	Hawthorn	0.09	0.06	0.02	14.84	10.87	3.97
	Hazel	0.05	0.04	0.01	10.39	8.84	1.54
	Red maple	0.04	0.04	0.00	10.19	9.78	0.41
	Sycamore	0.07	0.05	0.01	12.38	9.83	2.55
	Mean	0.06	0.05	0.01	11.57	9.38	2.19
PhotosynQ MultispeQ V1.0	Ash	0.09	0.05	0.04	16.19	8.83	7.36
	Beech	0.04	0.04	0.00	6.91	7.57	-0.66
	Silver birch	0.05	0.04	0.01	12.33	10.77	1.56
	Hawthorn	0.12	0.09	0.03	20.41	15.56	4.84
	Hazel	0.06	0.04	0.02	11.78	7.90	3.88
	Red maple	0.05	0.04	0.01	12.94	10.66	2.28
	Sycamore	0.07	0.05	0.02	13.01	9.17	3.83
	Mean	0.07	0.05	0.02	13.37	10.07	3.30

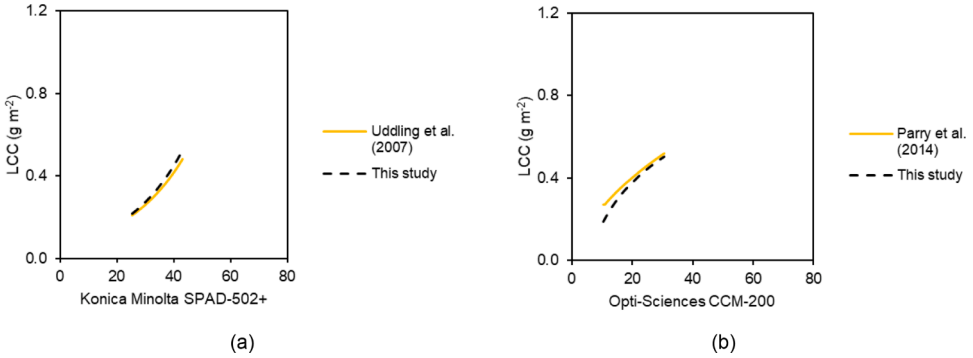

Fig. D1. Comparison of calibration functions for silver birch (*Betula pendula*) presented by Uddling et al. (2007) (a) and Parry et al. (2014) (b) against the calibration functions derived in this study for the same species. In the case of Parry et al. (2014), LCC was converted from mol m^{-2} to g m^{-2} according to Eq. (6).

finding nearly identical relationships for tomato, pepper, maize and pea leaves grown in greenhouse vs. outdoor environments. Additionally, in the same study, the chlorophyll meter – LCC relationship presented by Richardson et al. (2002) for paper birch (*Betula papyrifera*) seedlings grown in a greenhouse in Connecticut was found to closely match the relationship for mature trees using data from an outdoor arid environment in Utah over a decade later. Notably, our independently-derived calibration functions for silver birch (*Betula pendula*) were highly consistent with those presented by both Uddling et al. (2007) and Parry et al. (2014), providing further support to this suggestion (Appendix D).

4.3. Conversion between chlorophyll meter outputs

The fact that the relationships between the different chlorophyll meter outputs were very well described by simple linear, exponential, and logarithmic functions is encouraging, and suggests that by adopting such conversion functions, the different chlorophyll meters could be used interchangeably. For research teams with access to several different models, this is a useful finding that could facilitate more extensive data collection than if restricting to a single model. Additionally, the conversion functions described in this paper should prove useful in better enabling comparison with previous studies. This is a particularly important consideration if primary calibration data are not being collected, since a far greater number of calibration functions have been published for the Konica Minolta SPAD-502+ and Opti-Sciences CCM-200 than for the other investigated chlorophyll meters (Coste et al., 2010; Demarez et al., 1999; Markwell et al., 1995; Parry et al., 2014; Percival et al., 2008; Richardson et al., 2002; Steele et al., 2008; Uddling et al., 2007).

Whilst several functions have been published for converting between the outputs of the Konica Minolta SPAD-502+ and Opti-Sciences CCM-200 or atLEAF CHL PLUS instruments (Ali et al., 2021; Almansoori et al.,

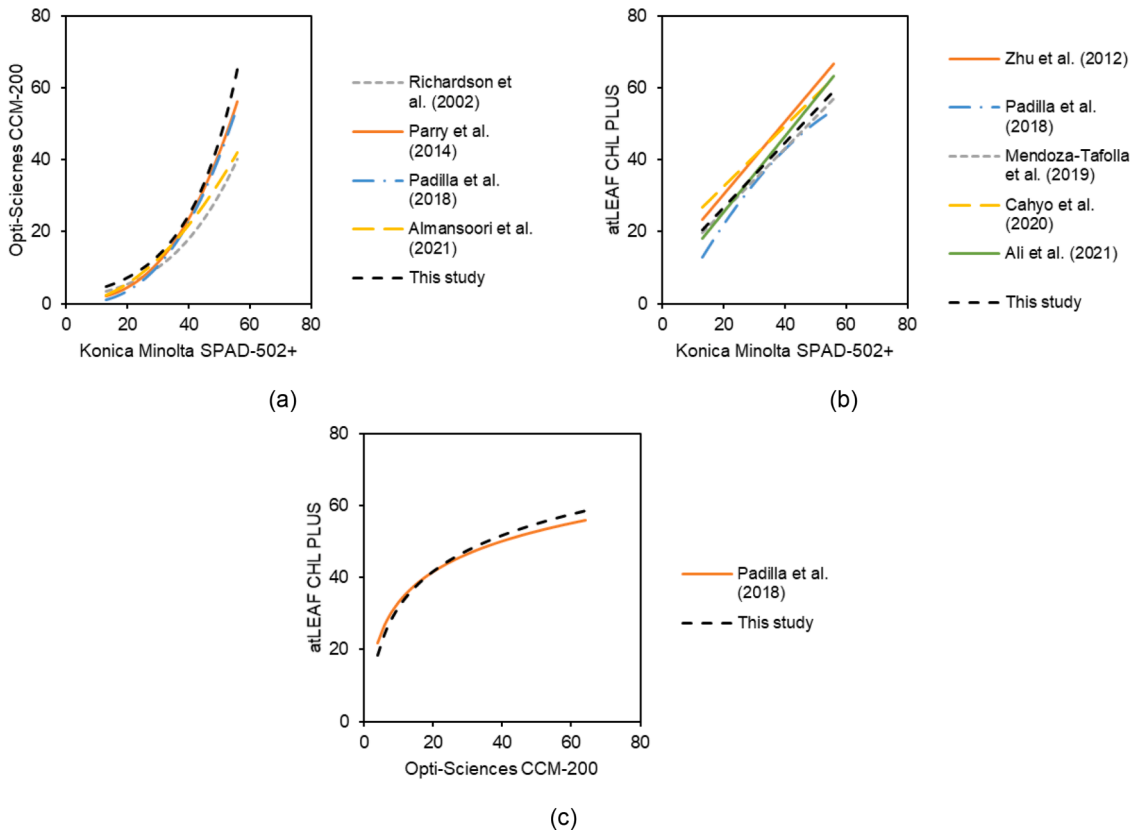

Fig. D2. Comparison of previously-published conversion functions to transform between chlorophyll meter outputs against the conversion functions derived in this study.

2021; Cahyo et al., 2020; Mendoza-Tafolla et al., 2019; Padilla et al., 2018; Parry et al., 2014; Richardson et al., 2002; Zhu et al., 2012), our study is the first to provide a comprehensive set of conversion functions for all four investigated models (albeit over a limited range of values). Notably, our results demonstrated good consistency with previously-published conversion functions (Appendix D), providing further confidence in their utility. When compared to the other chlorophyll meters, the step observed in the outputs of the PhotosynQ MultispeQ V1.0 at values of greater than 50 (Fig. 3) is likely related to the use of measurements at different light intensities (Kuhlgert et al., 2016). For leaves with greater LCC, higher light intensity measurements are likely to have been selected by the instrument, with the step representing the transition between measurements at higher and lower intensities.

4.4. Utility of transmittance spectroscopy and trade-offs between performance and practicality

We hypothesised that when compared to the investigated chlorophyll meters, the potentially higher quality, signal-to-noise, and sensitivity characteristics of the spectroradiometer would improve relationships with destructively-determined LCC. When calculated using the same wavelengths and measurement equations, our results revealed that the transmittance-based indices did not, in fact, provide stronger relationships with destructively-determined LCC than the chlorophyll meters themselves. It is worth noting that although the chlorophyll meter manufacturers quote central wavelength values for the incorporated LEDs, they likely have a different spectral response to the spectroradiometer, whose full width at half maximum (FWHM) is 3 nm (ASD, 2008). For example, the manual of the Konica Minolta SPAD-502+ presents a plot of 'relative luminous intensity' as a function of wavelength, in which the 650 nm and 940 nm LEDs are shown to have a FWHM of approximately 2 nm and 5 nm, respectively (Konica Minolta, 2009). These relatively small differences in spectral response could influence the degree of signal integrated (particularly in the red chlorophyll absorption feature at the base of the red-edge, where transmittance varies substantially according to wavelength – see Fig. 1), and might explain the reduced strength of the relationships observed in the case of the transmittance-based indices (Dian et al., 2016).

Our characterisation of the relationships between the transmittance-based indices and the outputs of the associated chlorophyll meters may represent useful information for those attempting to simulate chlorophyll meter outputs using modelled or measured transmittance spectra. For the Konica Minolta SPAD-502+, our estimated k and C coefficients (38.26 and -2.99) are in broad agreement with Hunt and Daughtry (2014), who estimated values of 37.0 and -2.68 using a series of plastic filters. It is worth noting that whilst previous studies have suggested the CCI index provided by the Opti-Sciences CCM-200 is equivalent to T_{931}/T_{653} (Parry et al., 2014), we did not observe a 1:1 relationship (indicated by k and C coefficients of approximately 1.68 and 0.83, respectively). Again, this discrepancy could be related to differences in the spectral response of the LEDs incorporated within the chlorophyll meters and that of the spectroradiometer adopted in this study.

Increases in the strength of the relationships between transmittance-based indices and destructively-determined LCC were achievable when all possible combinations of wavelengths were considered to identify optimal spectral bands, whilst for the full-spectrum approach involving PLSR, transmittance spectroscopy outperformed the chlorophyll meters, explaining an average of 10% more variation in LCC over all investigated cases and resulting in an average reduction in RMSE of 0.04 g m^{-2}. These findings are not surprising, since the chlorophyll meters (and the transmittance indices based on them) make use of only two fixed spectral bands and disregard information contained in other parts of the transmittance spectrum.

The fact that the optimal bands and largest PLSR coefficients were

associated with wavelengths not measured by the chlorophyll meters demonstrates that they may not exploit all relevant spectral information, such as that contained at blue and green wavelengths. Indeed, Gitelson et al. (1996) demonstrated that the relationship between absorption and LCC is less prone to saturation at green rather than red wavelengths, whilst information from the blue region has previously been used to improve the sensitivity of reflectance-based indices to LCC (Gitelson et al., 2003; Sims and Gamon, 2002). Given that there are known chlorophyll absorption features in the blue region of the spectrum (Curran, 1989; Ustin et al., 2009), the use of blue wavelengths has a clear physical basis (despite being typically avoided in remote sensing applications due to increased atmospheric scattering, which is not a concern for transmittance measurements at the leaf level).

Whilst not explicitly investigated in this study, a further potential application of transmittance spectroscopy is the discrimination of chlorophyll-a and -b, given that the absorption peaks of chlorophyll-a occur at slightly different wavelengths to chlorophyll-b (i.e. 430 nm and 662 nm, as opposed to 453 nm and 642 nm) (Curran, 1989; Ustin et al., 2009). These should be distinguishable thanks to the substantially increased spectral sampling when compared to two-band chlorophyll meters. Nevertheless, it is worth noting that previous studies have also demonstrated that chlorophyll-a and -b can be accurately estimated by simply establishing separate chlorophyll meter calibration functions for each component (i.e. $r^2 > 0.9$, RMSE < 0.03 g m^{-2}) (Richardson et al., 2002).

Despite its potential advantages, it should be noted that transmittance spectroscopy cannot match the ease of use of the chlorophyll meters, given the need to carry a spectroradiometer, computer, integrating sphere, and associated power supply into the field, and given the requirement for post-processing of the obtained raw data to derive transmittance and associated indices (Danner et al., 2015; Malthus et al., 2019; Milton et al., 2009; Suarez et al., 2015). Whilst somewhat more portable systems than that adopted in our study are available, such as the Ocean Optics Jazz SpectroClip (Grašič et al., 2021a, 2021b, 2019, 2017), such challenges are yet to be fully resolved. Excluding post-processing, a single measurement sequence with the spectroradiometer and integrating sphere took approximately 30 s, whereas a single chlorophyll meter measurement could be conducted in under 5 s. As such, there are clear trade-offs between accuracy and practicality that must be considered. For example, if the study site is heterogeneous, any increases in accuracy provided by transmittance spectroscopy may be negated by limited spatial sampling, as fewer measurements are likely to be possible for the same investment of time and effort. Likewise, the approach is less suited to the provision of near-real time information on vegetation status that may be required in agricultural and forest management applications.

5. Conclusions

Chlorophyll meters enable efficient and non-destructive in situ estimation of LCC, but their outputs represent a relative quantity, necessitating calibration against destructively-determined values to provide an absolute quantity that is comparable between different studies and species. We investigated the performance of the well-established Konica Minolta SPAD-502+ and Opti-Sciences CCM-200 instruments and the low-cost atLEAF CHL PLUS and PhotosynQ MultispeQ V1.0 devices for estimating LCC in eight temperate deciduous broadleaf forest species. Using the same leaf samples to ensure a fair comparison, we calibrated each chlorophyll meter against destructively-determined LCC, and characterised the relationships between the outputs of the different models. We also assessed whether transmittance spectroscopy could provide improvements in accuracy. Our results revealed that once calibrated, any of the investigated chlorophyll meters represent a suitable choice, with the low-cost devices demonstrating similar (and in some cases improved) performance to the well-established instruments. With the exception of oak, chlorophyll meter – LCC relationships were consistent between all investigated species, implying that for these species, generic calibration functions may be suitable depending on the required accuracy for the application at hand. LCC values provided by the generic calibration functions fell within the prediction uncertainties of species-specific calibration functions for most considered species, and use of the generic calibration functions led to a mean increase in RMSE (NRMSE) of just 0.01 g m^{-2} to 0.02 g m^{-2} (2% to 5%). Conversion functions between the different chlorophyll meters were presented, which will better facilitate comparison between studies adopting different models. Finally, increased performance was observed in the case of transmittance spectroscopy, indicating that the chlorophyll meters may not make use of all relevant spectral information (such as that contained at blue and green wavelengths), but improvements in accuracy need to be weighed against the reduced practicality of the approach in the field.

Declaration of Competing Interest

The authors declare that they have no known competing financial interests or personal relationships that could have appeared to influence the work reported in this paper.

Acknowledgements

The authors thank the two anonymous reviewers for their constructive comments, which helped to substantially improve the manuscript. This study has been undertaken using data from “Fiducial Reference Measurements for Vegetation – Phase 2” (FRM4VEG – Phase 2), which was funded by the European Space Agency. The authors thank the Natural Environment Research Council (NERC) Field Spectroscopy Facility (FSF) for supplying equipment and training that enabled a pilot study leading to this work.

Appendix

Appendix A. Variability of chlorophyll meter outputs at the leaf level

Fig. A1.

Appendix B. Association between leaf thickness and chlorophyll meter outputs

Significant correlations ($p < 0.05$) between leaf thickness and chlorophyll meter outputs were observed for all species except beech and oak, though these correlations were weak to moderate in all cases. Negative correlations were observed for the majority of species (r_s = -0.15 to -0.56), with the exception of beech and red maple, for which positive correlations were apparent (r_s = 0.10 to 0.14 for beech and r_s = 0.32 to 0.40 for red maple) (Table B1).

Appendix C. Comparison between generic and species-specific calibration functions

Fig. C1, Fig. C2, Fig. C3, Fig. C4, Table C1, Table C2

Appendix D. Comparison with previously-published calibration and conversion functions

Fig. D1 and Fig. D2

References

ADC Bioscientific, 2019. CCM-200 Plus Chlorophyll Content Meter. ADC Bioscientific, Hoddeson, United Kingdom.

Ali, A.K., Noraldeen, S.S., Yaseen, A.A., 2021. An evaluation study for chlorophyll estimation techniques. Sarhad J. Agric. 37 (4), 1458–1465. https://doi.org/10.17582/journal.sja/2021/37.4.1458.1465.

Almansoori, T., Majeda, S., Aljazeri, M., 2021. Rapid and nondestructive estimations of chlorophyll concentration in date palm (Phoenix dactylifera L.) leaflets using SPAD-502+ and CCM-200 portable chlorophyll meters. Emirates J. Food Agric. 33, 532–543. https://doi.org/10.9755/ejfa.2021.v33.i7.2723.

Apogee Instruments, 2020. Chlorophyll Conctentation Meter Owner's Manual, 28th-Oct-20, 2nd Ed. Apogee Instruments, Logan, Utah, United States.

ASD, 2008. FieldSpec 3 User Manual. Analytical Spectral Devices, Boulder, Colorado, United States.

Asner, G.P., Martin, R.E., Knapp, D.E., Tupayachi, R., Anderson, C., Carranza, L., Martinez, P., Houcheime, M., Sinca, F., Weiss, P., 2011. Spectroscopy of canopy chemicals in humid tropical forests. Remote Sens. Environ. 115, 3587–3598. https://doi.org/10.1016/j.rse.2011.08.020.

Atkins, J.W., Stovall, A.E.L., Yang, X., 2020. Mapping temperate forest phenology using tower, UAV, and ground-based sensors. Drones 4, 56. https://doi.org/10.3390/drones4030056.

Atzberger, C., Guérif, M., Baret, F., Werner, W., 2010. Comparative analysis of three chemometric techniques for the spectroradiometric assessment of canopy chlorophyll content in winter wheat. Comput. Electron. Agric. 73, 165–173. https://doi.org/10.1016/j.compag.2010.05.006.

Berra, E.F., Gaulton, R., Barr, S., 2017. Commercial off-the-shelf digital cameras on unmanned aerial vehicles for multitemporal monitoring of vegetation reflectance and NDVI. IEEE Trans. Geosci. Remote Sens. 55, 4878–4886. https://doi.org/10.1109/TGRS.2017.2655365.

Blackmer, T.M., Schepers, J.S., 1995. Use of a chlorophyll meter to monitor nitrogen status and schedule fertigation for corn. J. Prod. Agric. 8, 56–60. https://doi.org/10.2134/jpa1995.0056.

Bonneville, M., Fyles, J.W., 2006. Assessing variations in SPAD-502 chlorophyll meter measurements and their relationships with nutrient content of trembling aspen foliage. Commun. Soil Sci. Plant Anal. 37, 525–539. https://doi.org/10.1080/00103620500449385.

Brown, L.A., Camacho, F., García-Santos, V., Origo, N., Fuster, B., Morris, H., Pastor-Guzman, J., Sánchez-Zapero, J., Morrone, R., Ryder, J., Nightingale, J., Boccia, V., Dash, J., 2021. Fiducial reference measurements for vegetation bio-geophysical variables: an end-to-end uncertainty evaluation framework. Remote Sens. 13, 3194. https://doi.org/10.3390/rs13163194.

Burnett, A.C., Anderson, J., Davidson, K.J., Ely, K.S., Lamour, J., Li, Q., Morrison, B.D., Yang, D., Rogers, A., Serbin, S.P., 2021. A best-practice guide to predicting plant traits from leaf-level hyperspectral data using partial least squares regression. J. Exp. Bot. 72, 6175–6189. https://doi.org/10.1093/jxb/erab295.

Cahyo, A.N., Murti, R.H., Putra, E.T.S., Nuringtyas, T.R., Fabre, D., Montoro, P., 2020. SPAD-502 and atLEAF CHL PLUS values provide good estimation of the chlorophyll content for Hevea brasiliensis Müll. Arg. Leaves. E-J. Menara Perkeb. 88, 1–8. https://doi.org/10.22302/iribb.jur.mp.v88i1.369.

Carter, G.A., Knapp, A.K., 2001. Leaf optical properties in higher plants: linking spectral characteristics to stress and chlorophyll concentration. Am. J. Bot. 88, 677–684. https://doi.org/10.2307/2657068.

Cerovic, Z.G., Masdoumier, G., Ghozlen, N.Ben, Latouche, G., 2012. A new optical leaf-clip meter for simultaneous non-destructive assessment of leaf chlorophyll and epidermal flavonoids. Physiol. Plant 146, 251–260. https://doi.org/10.1111/j.1399-3054.2012.01639.x.

Chavana-Bryant, C., Malhi, Y., Wu, J., Asner, G.P., Anastasiou, A., Enquist, B.J., Cosio Caravasi, E.G., Doughty, C.E., Saleska, S.R., Martin, R.E., Gerard, F.F., 2017. Leaf aging of Amazonian canopy trees as revealed by spectral and physiochemical measurements. New Phytol. 214, 1049–1063. https://doi.org/10.1111/nph.13853.

Claverie, M., Ju, J., Masek, J.G., Dungan, J.L., Vermote, E.F., Roger, J.-C., Skakun, S.V., Justice, C., 2018. The harmonized Landsat and Sentinel-2 surface reflectance data set. Remote Sens. Environ. 219, 145–161. https://doi.org/10.1016/j.rse.2018.09.002.

Clevers, J.G.P.W., Gitelson, A.A., 2013. Remote estimation of crop and grass chlorophyll and nitrogen content using red-edge bands on Sentinel-2 and -3. Int. J. Appl. Earth Obs. Geoinf. 23, 344–351. https://doi.org/10.1016/j.jag.2012.10.008.

Coste, S., Baraloto, C., Leroy, C., Marcon, É., Renaud, A., Richardson, A.D., Roggy, J.-C., Schimann, H., Uddling, J., Hérault, B., 2010. Assessing foliar chlorophyll contents with the SPAD-502 chlorophyll meter: a calibration test with thirteen tree species of tropical rainforest in French Guiana. Ann. For. Sci. 67 https://doi.org/10.1051/forest/2010020, 607–607.

Curran, P.J., 1989. Remote sensing of foliar chemistry. Remote Sens. Environ. 30, 271–278. https://doi.org/10.1016/0034-4257(89)90069-2.

Danner, M., Locherer, M., Hank, T., Richter, K., 2015. EnMAP Field Guides: Technical Report: Spectral Sampling with the ASD FIELDSPEC 4. GeoForschungsZentrum Data Services, Potsdam, Germany.

Darvishzadeh, R., Atzberger, C., Skidmore, A., Schlerf, M., 2011. Mapping grassland leaf area index with airborne hyperspectral imagery: A comparison study of statistical approaches and inversion of radiative transfer models. ISPRS J. Photogramm. Remote Sens. 66, 894–906. https://doi.org/10.1016/j.isprsjprs.2011.09.013.

Dash, J., Curran, P.J., Tallis, M.J., Llewellyn, G.M., Taylor, G., Snoeij, P., 2010. Validating the MERIS Terrestrial Chlorophyll Index (MTCI) with ground chlorophyll content data at MERIS spatial resolution. Int. J. Remote Sens. 31, 5513–5532. https://doi.org/10.1080/01431160903376340.

Demarez, V., Gastellu-Etchegorry, J.P., Mougin, E., Marty, G., C, P., Dufrêne, E., Le Dantec, V., 1999. Seasonal variation of leaf chlorophyll content of a temperate forest. Inversion of the PROSPECT model. Int. J. Remote Sens. 20, 879–894. https://doi.org/10.1080/014311699212975.

Dian, Y., Le, Y., Fang, S., Xu, Y., Yao, C., Liu, G., 2016. Influence of spectral bandwidth and position on chlorophyll content retrieval at leaf and canopy levels. J. Indian Soc. Remote Sens. 44, 583–593. https://doi.org/10.1007/s12524-015-0537-2.

Dillen, S.Y., de Beeck, M.O., Hufkens, K., Buonanduci, M., Phillips, N.G., 2012. Seasonal patterns of foliar reflectance in relation to photosynthetic capacity and color index in two co-occurring tree species, Quercus rubra and Betula papyrifera. Agric. For. Meteorol. 160, 60–68. https://doi.org/10.1016/j.agrformet.2012.03.001.

Dong, T., Shang, J., Chen, J.M., Liu, J., Qian, B., Ma, B., Morrison, M.J., Zhang, C., Liu, Y., Shi, Y., Pan, H., Zhou, G., 2019. Assessment of portable chlorophyll meters for measuring crop leaf chlorophyll concentration. Remote Sens. 11, 2706. https://doi.org/10.3390/rs11222706.

Fawcett, D., Panigada, C., Tagliabue, G., Boschetti, M., Celesti, M., Evdokimov, A., Biriukova, K., Colombo, R., Miglietta, F., Rascher, U., Anderson, K., 2020. Multi-scale evaluation of drone-based multispectral surface reflectance and vegetation indices in operational conditions. Remote Sens. 12, 514. https://doi.org/10.3390/rs12030514.

Féret, J.-B., François, C., Gitelson, A., Asner, G.P., Barry, K.M., Panigada, C., Richardson, A.D., Jacquemoud, S., 2011. Optimizing spectral indices and chemometric analysis of leaf chemical properties using radiative transfer modeling. Remote Sens. Environ. 115, 2742–2750. https://doi.org/10.1016/j.rse.2011.06.016.

FT Green, 2018. atLEAF+ Chlorophyll Meter User Manual, 1.0 Ed. FT Green, Wilmington, Delaware, United States, p. 1.0. ed..

Gamon, J.A., Cheng, Y., Claudio, H., MacKinney, L., Sims, D.A., 2006a. A mobile tram system for systematic sampling of ecosystem optical properties. Remote Sens. Environ. 103, 246–254. https://doi.org/10.1016/j.rse.2006.04.006.

Gamon, J.A., Rahman, A.F., Dungan, J.L., Schildhauer, M., Huemmrich, K.F., 2006b. Spectral Network (SpecNet)-What is it and why do we need it? Remote Sens. Environ. 103, 227–235. https://doi.org/10.1016/j.rse.2006.04.003.

Gao, B.-C., Montes, M.J., Davis, C.O., Goetz, A.F.H., 2009. Atmospheric correction algorithms for hyperspectral remote sensing data of land and ocean. Remote Sens. Environ. 113, S17–S24. https://doi.org/10.1016/j.rse.2007.12.015.

Gitelson, A.A., Buschmann, C., Lichtenthaler, H.K., 1999. The chlorophyll fluorescence ratio F735/F700 as an accurate measure of the chlorophyll content in plants. Remote Sens. Environ. 69, 296–302. https://doi.org/10.1016/S0034-4257(99)00023-1.

Gitelson, A.A., Gritz, Y., Merzlyak, M.N., 2003. Relationships between leaf chlorophyll content and spectral reflectance and algorithms for non-destructive chlorophyll assessment in higher plant leaves. J. Plant Physiol. 160, 271–282. https://doi.org/10.1078/0176-1617-00887.

Gitelson, A.A., Kaufman, Y.J., Merzlyak, M.N., 1996. Use of a green channel in remote sensing of global vegetation from EOS-MODIS. Remote Sens. Environ. 58, 289–298. https://doi.org/10.1016/S0034-4257(96)00072-7.

Grašič, M., Budak, V., Klančnik, K., Gaberščik, A., 2017. Optical properties of halophyte leaves are affected by the presence of salt on the leaf surface. Biologia 72, 1131–1139. https://doi.org/10.1515/biolog-2017-0125.

Grašič, M., Dacar, M., Gaberščik, A., 2021a. Comparative study of temporal changes in pigments and optical properties in sepals of Helleborus odorus and H. niger from prebloom to seed production. Plants 11, 119. https://doi.org/10.3390/plants11010119.

Grašič, M., Piberčnik, M., Zelnik, I., Abram, D., Gaberščik, A., 2019. Invasive alien vines affect leaf traits of riparian woody vegetation. Water 11, 2395. https://doi.org/10.3390/w11112395.

Grašič, M., Planinc, G., Gaberščik, A., 2021b. Bracts and basal leaves in Hacquetia epipactis differ in their spectral signatures. Biologia 76, 831–840. https://doi.org/10.2478/s11756-020-00650-4.

Hansen, P.M., Schjoerring, J.K., 2003. Reflectance measurement of canopy biomass and nitrogen status in wheat crops using normalized difference vegetation indices and partial least squares regression. Remote Sens. Environ. 86, 542–553. https://doi.org/10.1016/S0034-4257(03)00131-7.

Herrmann, I., Pimstein, A., Karnieli, A., Cohen, Y., Alchanatis, V., Bonfil, D.J., 2011. LAI assessment of wheat and potato crops by VENμS and Sentinel-2 bands. Remote Sens. Environ. 115, 2141–2151. https://doi.org/10.1016/j.rse.2011.04.018.

Hilker, T., Coops, N.C., Nesic, Z., Wulder, M.A., Black, A.T., 2007. Instrumentation and approach for unattended year round tower based measurements of spectral reflectance. Comput. Electron. Agric. 56, 72–84. https://doi.org/10.1016/j.compag.2007.01.003.

Hill, J., Buddenbaum, H., Townsend, P.A., 2019. Imaging spectroscopy of forest ecosystems: perspectives for the use of space-borne hyperspectral earth observation systems. Surv. Geophys. 40, 553–588. https://doi.org/10.1007/s10712-019-09514-2.

Hunt, E.R., Daughtry, C.S.T., 2014. Chlorophyll meter calibrations for chlorophyll content using measured and simulated leaf transmittances. Agron. J. 106, 931–939. https://doi.org/10.2134/agronj13.0322.

Koike, T., 1990. Autumn coloring, photosynthetic performance and leaf development of deciduous broad-leaved trees in relation to forest succession. Tree Physiol 7, 21–32. https://doi.org/10.1093/treephys/7.1-2-3-4.21.

Konica Minolta, 2009. Chlorophyll Meter SPAD-502Plus Instruction Manual. Konica Minolta, Osaka, Japan.

Kuhlgert, S., Austic, G., Zegarac, R., Osei-Bonsu, I., Hoh, D., Chilvers, M.I., Roth, M.G., Bi, K., TerAvest, D., Weebadde, P., Kramer, D.M., 2016. MultispeQ Beta: a tool for large-scale plant phenotyping connected to the open PhotosynQ network. R. Soc. Open Sci. 3, 160592 https://doi.org/10.1098/rsos.160592.

le Maire, G., François, C., Soudani, K., Berveiller, D., Pontailler, J.Y., Bréda, N., Genet, H., Davi, H., Dufrêne, E., 2008. Calibration and validation of hyperspectral indices for the estimation of broadleaved forest leaf chlorophyll content, leaf mass per area, leaf area index and leaf canopy biomass. Remote Sens. Environ. 112, 3846–3864. https://doi.org/10.1016/j.rse.2008.06.005.

Leuning, R., Hughes, D., Daniel, P., Coops, N.C., Newnham, G., 2006. A multi-angle spectrometer for automatic measurement of plant canopy reflectance spectra. Remote Sens. Environ. 103, 236–245. https://doi.org/10.1016/j.rse.2005.06.016.

Lhotáková, Z., Albrechtová, J., Malenovský, Z., Rock, B.N., Polák, T., Cudlín, P., 2007. Does the azimuth orientation of Norway spruce (Picea abies/L./Karst.) branches within sunlit crown part influence the heterogeneity of biochemical, structural and spectral characteristics of needles? Environ. Exp. Bot. 59, 283–292. https://doi.org/10.1016/j.envexpbot.2006.02.003.

LI-COR, 1988. 1800-12 Intergrating Sphere Instruction Manual. LI-COR, Lincoln, Nebraska, United States.

Lichtenthaler, H.K., Wenzel, O., Buschmann, C., Gitelson, A., 1998. Plant stress detection by reflectance and fluorescence. Ann. NY Acad. Sci. 851, 271–285. https://doi.org/10.1111/j.1749-6632.1998.tb09002.x.

Malthus, T., Ong, C., Lau, I., Fearns, P., Byrne, G., Thankappan, M., Chisholm, L., Suarez, L., Clarke, K., Scarth, P., Phinn, S., 2019. A Community Approach to the Standardised Validation of Surface Reflectance Data, 2.0. ed. Commonwealth Scientific and Industrial Research Organisation, Canberra, Australia.

Markwell, J., Osterman, J.C., Mitchell, J.L., 1995. Calibration of the Minolta SPAD-502 leaf chlorophyll meter. Photosynth. Res. 46, 467–472. https://doi.org/10.1007/BF00032301.

Mendoza-Tafolla, R.O., Juarez-Lopez, P., Ontiveros-Capurata, R.E., Sandoval-Villa, M., Alia-Tejacal, I., Alejo-Santiago, G., 2019. Estimating nitrogen and chlorophyll status of romaine lettuce using SPAD and at LEAF readings. Not. Bot. Horti Agrobot. Cluj-Napoca 47, 751–756. https://doi.org/10.15835/nbha47311589.

Meroni, M., Barducci, A., Cogliati, S., Castagnoli, F., Rossini, M., Busetto, L., Migliavacca, M., Cremonese, E., Galvagno, M., Colombo, R., di Cella, U.M., 2011. The hyperspectral irradiometer, a new instrument for long-term and unattended field spectroscopy measurements. Rev. Sci. Instrum. 82, 043106 https://doi.org/10.1063/1.3574360.

Milton, E.J., Schaepman, M.E., Anderson, K., Kneubühler, M., Fox, N., 2009. Progress in field spectroscopy. Remote Sens. Environ. 113, S92–S109. https://doi.org/10.1016/j.rse.2007.08.001.

Moncholi-Estornell, A., Van Wittenberghe, S., Cendrero-Mateo, M.P., Alonso, L., Malenovský, Z., Moreno, J., 2021. Impact of structural, photochemical and instrumental effects on leaf and canopy reflectance variability in the 500–600 nm range. Remote Sens 14, 56. https://doi.org/10.3390/rs14010056.

Monje, O.A., Bugbee, B., 1992. Inherent limitations of nondestructive chlorophyll meters: a comparison of two types of meters. HortScience 27, 69–71. https://doi.org/10.21273/HORTSCI.27.1.69.

Nauš, J., Prokopová, J., Řebíček, J., Špundová, M., 2010. SPAD chlorophyll meter reading can be pronouncedly affected by chloroplast movement. Photosynth. Res. 105, 265–271. https://doi.org/10.1007/s11120-010-9587-z.

Newman, G., Wiggins, A., Crall, A., Graham, E., Newman, S., Crowston, K., 2012. The future of citizen science: emerging technologies and shifting paradigms. Front. Ecol. Environ. 10, 298–304. https://doi.org/10.1890/110294.

Noda, H.M., Muraoka, H., Nasahara, K.N., 2021. Phenology of leaf optical properties and their relationship to mesophyll development in cool-temperate deciduous broad-leaf trees. Agric. For. Meteorol. 297, 108236 https://doi.org/10.1016/j.agrformet.2020.108236.

Origo, N., Gorroño, J., Ryder, J., Nightingale, J., Bialek, A., 2020. Fiducial reference measurements for validation of Sentinel-2 and Proba-V surface reflectance products. Remote Sens. Environ. 241, 111690 https://doi.org/10.1016/j.rse.2020.111690.

Padilla, F.M., de Souza, R., Peña-Fleitas, M.T., Gallardo, M., Giménez, C., Thompson, R. B., 2018. Different responses of various chlorophyll meters to increasing nitrogen supply in sweet pepper. Front. Plant Sci. 9, 1–14. https://doi.org/10.3389/fpls.2018.01752.

Parry, C., Blonquist, J.M., Bugbee, B., 2014. In situ measurement of leaf chlorophyll concentration: analysis of the optical/absolute relationship. Plant. Cell Environ. 37, 2508–2520. https://doi.org/10.1111/pce.12324.

Peng, S., Garcia, F.V., Laza, R.C., Sanico, A.L., Visperas, R.M., Cassman, K.G., 1996. Increased N-use efficiency using a chlorophyll meter on high-yielding irrigated rice. F. Crop. Res. 47, 243–252. https://doi.org/10.1016/0378-4290(96)00018-4, 10.1016/0378-4290(96)00018-4.

Percival, G.C., Keary, I.P., Noviss, K., 2008. The potential of a chlorophyll content SPAD meter to quantify nutrient stress in foliar tissue of sycamore (Acer pseudoplatanus), English oak (Quercus robur), and European beech (Fagus sylvatica). Arboric. Urban For. 34, 89–100. https://doi.org/10.48044/jauf.2008.012.

PhotosynQ, 2021a. MultispeQ v1.0 [WWW Document]. URL https://help.photosynq.com/instruments/multispeq-v1.0.html#configuration (accessed 10.7.21).

PhotosynQ, 2021b. MultispeQ v2.0 [WWW Document]. URL https://help.photoshttps//help.photosynq.com/instruments/multispeq-v2.0.html#configuration (accessed 3.7.22).

Revill, A., Florence, A., MacArthur, A., Hoad, S., Rees, R., Williams, M., 2019. The value of Sentinel-2 spectral bands for the assessment of winter wheat growth and development. Remote Sens. 11, 2050. https://doi.org/10.3390/rs11172050.

Richardson, A.D., Duigan, S.P., Berlyn, G.P., 2002. An evaluation of noninvasive methods to estimate foliar chlorophyll content. New Phytol. 153, 185–194. https://doi.org/10.1046/j.0028-646X.2001.00289.x.

Sakowska, K., Gianelle, D., Zaldei, A., MacArthur, A., Carotenuto, F., Miglietta, F., Zampedri, R., Cavagna, M., Vescovo, L., 2015. WhiteRef: a new tower-based hyperspectral system for continuous reflectance measurements. Sensors 15, 1088–1105. https://doi.org/10.3390/s150101088.

Sakowska, K., Juszczak, R., Gianelle, D., 2016. Remote sensing of grassland biophysical parameters in the context of the Sentinel-2 satellite mission. J. Sensors 2016, 1–16. https://doi.org/10.1155/2016/4612809.

Sims, D.A., Gamon, J.A., 2002. Relationships between leaf pigment content and spectral reflectance across a wide range of species, leaf structures and developmental stages. Remote Sens. Environ. 81, 337–354. https://doi.org/10.1016/S0034-4257(02)00010-X.

Spafford, L., le Maire, G., MacDougall, A., de Boissieu, F., Féret, J.-B., 2021. Spectral subdomains and prior estimation of leaf structure improves PROSPECT inversion on reflectance or transmittance alone. Remote Sens. Environ. 252, 112176 https://doi.org/10.1016/j.rse.2020.112176.

Spectrum Technologies, 2009. SPAD 502DL Plus Chlorophyll Meter Data Logger Manual. Spectrum Technologies, Aurora, Illinois, United States.

Steele, M.R., Gitelson, A.A., Rundquist, D.C., 2008. A comparison of two techniques for nondestructive measurement of chlorophyll content in grapevine leaves. Agron. J. 100, 779. https://doi.org/10.2134/agronj2007.0254N.

Suarez, L., Restrepo-Coupe, N., Hueni, A., Chisholm, L.A., 2015. Vegetation spectroscopy. In: Held, A., Phinn, S., Soto-Berelov, M., Jones, S. (Eds.), Review of Validation Standards of Biophysical Earth Observation Products. Terrestrial Ecosystem Research Network, St Lucia, Australia, pp. 221–233.

Sun, J., Shi, S., Yang, J., Du, L., Gong, W., Chen, B., Song, S., 2018. Analyzing the performance of PROSPECT model inversion based on different spectral information for leaf biochemical properties retrieval. ISPRS J. Photogramm. Remote Sens. 135, 74–83. https://doi.org/10.1016/j.isprsjprs.2017.11.010.

Tagesson, T., Fensholt, R., Huber, S., Horion, S., Guiro, I., Ehammer, A., Ardö, J., 2015. Deriving seasonal dynamics in ecosystem properties of semi-arid savanna grasslands from in situ-based hyperspectral reflectance. Biogeosciences 12, 4621–4635. https://doi.org/10.5194/bg-12-4621-2015.

Thompson, D.R., Gao, B.-C., Green, R.O., Roberts, D.A., Dennison, P.E., Lundeen, S.R., 2015. Atmospheric correction for global mapping spectroscopy: ATREM advances for the HyspIRI preparatory campaign. Remote Sens. Environ. 167, 64–77. https://doi.org/10.1016/j.rse.2015.02.010.

Uddling, J., Gelang-Alfredsson, J., Piikki, K., Pleijel, H., 2007. Evaluating the relationship between leaf chlorophyll concentration and SPAD-502 chlorophyll meter readings. Photosynth. Res. 91, 37–46. https://doi.org/10.1007/s11120-006-9077-5.

Upreti, D., Huang, W., Kong, W., Pascucci, S., Pignatti, S., Zhou, X., Ye, H., Casa, R., 2019. A comparison of hybrid machine learning algorithms for the retrieval of wheat biophysical variables from Sentinel-2. Remote Sens 11, 481. https://doi.org/10.3390/rs11050481.

Ustin, S.L., Gitelson, A.A., Jacquemoud, S., Schaepman, M., Asner, G.P., Gamon, J.A., Zarco-Tejada, P., 2009. Retrieval of foliar information about plant pigment systems from high resolution spectroscopy. Remote Sens. Environ. 113, S67–S77. https://doi.org/10.1016/j.rse.2008.10.019.

van den Berg, A.K., Perkins, T.D., 2004. Evaluation of a portable chlorophyll meter to estimate chlorophyll and nitrogen contents in sugar maple (Acer saccharum Marsh.) leaves. For. Ecol. Manage 200, 113–117. https://doi.org/10.1016/j.foreco.2004.06.005.

Varvel, G.E., Schepers, J.S., Francis, D.D., 1997. Ability for in-season correction of nitrogen deficiency in corn using chlorophyll meters. Soil Sci. Soc. Am. J. 61, 1233–1239. https://doi.org/10.2136/sssaj1997.03615995006100040032x.

Vermote, E., Justice, C., Claverie, M., Franch, B., 2016. Preliminary analysis of the performance of the Landsat 8/OLI land surface reflectance product. Remote Sens. Environ. 185, 46–56. https://doi.org/10.1016/j.rse.2016.04.008.

Wang, J.F., He, D.X., Song, J.X., Dou, H.J., Du, W.F., 2015. Non-destructive measurement of chlorophyll in tomato leaves using spectral transmittance. Int. J. Agric. Biol. Eng. 8, 73–78. https://doi.org/10.3965/j.ijabe.20150805.1931.

Wang, R., Gamon, J.A., Moore, R., Zygielbaum, A.I., Arkebauer, T.J., Perk, R., Leavitt, B., Cogliati, S., Wardlow, B., Qi, Y., 2021. Errors associated with atmospheric correction methods for airborne imaging spectroscopy: Implications for vegetation indices and plant traits. Remote Sens. Environ. 265, 112663 https://doi.org/10.1016/j.rse.2021.112663.

Wang, Z., Chlus, A., Geygan, R., Ye, Z., Zheng, T., Singh, A., Couture, J.J., Cavender-Bares, J., Kruger, E.L., Townsend, P.A., 2020. Foliar functional traits from imaging spectroscopy across biomes in eastern North America. New Phytol. 228, 494–511. https://doi.org/10.1111/nph.16711.

Wellburn, A.R., 1994. The spectral determination of chlorophylls a and b, as well as total carotenoids, using various solvents with spectrophotometers of different resolution. J. Plant Physiol. 144, 307–313. https://doi.org/10.1016/S0176-1617(11)81192-2.

Wolters, E., Toté, C., Sterckx, S., Adriaensen, S., Henocq, C., Bruniquel, J., Scifoni, S., Dransfeld, S., 2021. iCOR atmospheric correction on Sentinel-3/OLCI over land: intercomparison with AERONET, RadCalNet, and SYN Level-2. Remote Sens. 13, 654. https://doi.org/10.3390/rs13040654.

Woodgate, W., van Gorsel, E., Hughes, D., Suarez, L., Jimenez-Berni, J., Held, A., 2020. THEMS: an automated thermal and hyperspectral proximal sensing system for canopy reflectance, radiance and temperature. Plant Methods 16, 105. https://doi.org/10.1186/s13007-020-00646-w.

Yamada, N., Fujimura, S., 1991. Nondestructive measurement of chlorophyll pigment content in plant leaves from three-color reflectance and transmittance. Appl. Opt. 30, 3964. https://doi.org/10.1364/AO.30.003964.

Zhu, J., Tremblay, N., Liang, Y., 2012. Comparing SPAD and atLEAF values for chlorophyll assessment in crop species. Can. J. Soil Sci. 92, 645–648. https://doi.org/10.4141/cjss2011-100.